CHAPTER

# 9

# Polytopic Models for Observer and Fault-Tolerant Control Designs

*Rodolfo Orjuela*[*], *Dalil Ichalal*[†], *Benoît Marx*[‡], *Didier Maquin*[‡], *José Ragot*[‡]

**[*]IRIMAS, Université de Haute-Alsace, 68093, Mulhouse, France [†]IBISC, Univ Evry, Université Paris Saclay, 91020 Courcouronnes, France [‡]CRAN, Université de Lorraine-CNRS, 54000 Nancy, France**

Control engineers must constantly cope with new technological challenges to increase system performance and reliability, as well as users' safety. Model-based automatic control is often employed to meet these objectives, and then one must use mathematical models to describe the system behaviors. On one hand, these models must accurately represent the real system behaviors, and on the other hand, they must be practically tractable. Usually, the mathematical model complexity increases with the complexity of the physical phenomena to be captured, naturally reducing its ease of use. As a result, a trade-off between precision and simplicity must be made. Several models with different mathematical structures are proposed to cope with the modeling of complex systems. Among these models, polytopic models (PMs), also known as linear parameter varying (LPV) model [1], multiple model (MM) [2], or Takagi-Sugeno (TS) model [3], are able to accurately describe these behaviors in a large operating range with an appropriate mathematical structure for automatic control purposes (modeling, stability analysis, state estimation, control).

Roughly speaking, the PM approach can be viewed as a smooth interpolation, using appropriate weighting functions, between a set of linear time


https://doi.org/10.1016/B978-0-12-817038-0.00009-3

invariant (LTI) models. In the PM framework, the mathematical system modeling is carried out through a decomposition of the system operating space into several operating areas, and the nonlinear system behavior into each operating area is then modeled, thanks to a linear submodel as described in [4–9], and for a recent review, in [10, 11]. Even if it is not the most efficient way to obtain a PM, an intuitive vision of the PM approach is to imagine that the LTI models could be obtained by linearizing the nonlinear system at given points, and the interpolation would be made according to the distances from the operating point to these linearization points. The aggregation of these submodels, with the help of the weighting functions, generates the PM representation of the considered system, and consequently a single nonlinear model is replaced by a set of linear submodels with an interpolation mechanism. By appropriately choosing the number of submodels and the weighting functions, a large class of nonlinear models can be represented with the PM structure. Therefore, the PM approach offers also a generic way, allowing us to capture the nonlinear system behavior in a large operating range, as shown later in this chapter.

The polytopic modeling problem can be summarized as how the operating space can be decomposed, and how the linear submodels can be obtained. Answers to these questions are provided in a black-box modeling approach from an experimental input/output data system using appropriate identification techniques [3, 9, 12, 13], or in a white-box modeling approach, from the nonlinear equations describing the system phenomena [14–16] as presented in this chapter. Because the interpolation between submodels is time-varying, the whole PM is a nonlinear model with a particular structure reducing the complexity analysis. In fact, with the interpolated submodels being linear, and the weighting functions satisfying the so-called convex sum properties, some well-known and efficient tools inspired of the linear system theory can be extended to nonlinear systems represented by PMs without a specific analysis of nonlinearities.

Polytopic modeling is the backbone of all concepts presented in this chapter, beginning with the stability analysis. Indeed, stability conditions for PMs are a generalization of linear system stability conditions. As shown in the next sections, stability conditions for PMs under a linear matrix inequality (LMI) formulation can be obtained using the Lyapunov theory [17–23]. These stability conditions are useful, and constitute the starting point to controller design [18, 24, 25] and observer synthesis [6, 26–30] for nonlinear systems represented by a PM. The state feedback controller design problem is addressed by providing stability conditions of the closed-loop system under an LMI form. When the state variables of the system are not measurable, observer-based state estimation is often needed, and therefore, some observer designs are also presented in this

chapter; for example, when unknown inputs (UIs), such as actuator faults, act on the system. Pole clustering under LMI conditions allowing dynamic performance, as well as disturbance attenuation conditions, are also presented. Finally, state feedback and state observer designs are combined in a single architecture to obtain an active fault-tolerant control (FTC) to preserve the closed-loop stability and performances of the system, even if some faults affect the system components, for example: sensors, actuators, or internal components.

According to the foregoing, the purpose of this chapter is to provide a short overview on the use of the PM approach to cope with the modeling, stability analysis, state feedback, state observer, and FTC of nonlinear systems. Indeed, PMs offer interesting mathematical, as well as practical, properties:

1. A large class of nonlinear dynamic systems with bounded nonlinearities, at least on a compact set of the state space, can be exactly written as a PM in a large operating range.
2. The specific analysis of nonlinearities of the investigated system is avoided thanks to the mathematical structure of the PMs, where the submodels are linear and the nonlinearities are rejected in the weighting functions, ensuring convex sum properties.
3. The use of PMs is interesting to extend tools developed in the linear framework to investigate stability/performance analysis and controller/observer design for nonlinear systems represented by PM.
4. The PM approach offers a large operating range of validity particularity needed in the FTC framework, because the fault incidence may deviate the system from its nominal operating point.

Due to these appealing properties of the PM approach, it is used in many engineering fields. One may cite the automotive applications, such as constraints control in [31] or the vehicle lateral dynamics estimation in experimental conditions [32]. The PM approach is successfully employed in [25, 33] to show a modeling application of a waste-water treatment plant, or in wind turbine estimation and control [34, 35]. In [36], the PM approach is also used to model a flexible one-link robot.

The outline of this chapter is illustrated in Fig. 9.1. Section 1, dedicated to the polytopic modeling, is the starting point of all the further developments. Based on this mathematical form, the stability analysis of PMs is addressed in Section 2. Some sufficient stability conditions are given in the LMI formalism, and illustrated. Thanks to these stability conditions, robust state feedback control design and state and UI observer design, are, respectively, detailed in Sections 3 and 4. All these materials are steps to propose, in Section 5, an FTC strategy. This FTC design is applied in simulation to address the lateral stabilization of a vehicle.

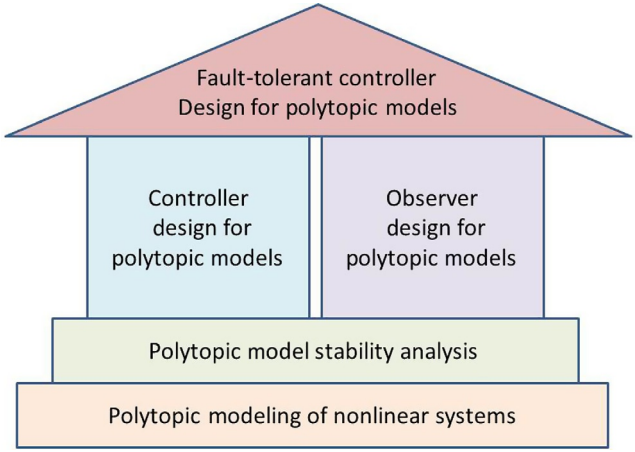


**FIG. 9.1** Scope of the chapter.

## 1 POLYTOPIC MODEL-BASED MODELING

Nonlinear models describing real systems may be obtained from physical laws, such as energy conservation, chemical kinetics, or from measured data-based identification. In the first case, using a white-box approach, the obtained model is often nonlinear, and too complex to be used in controller or observer designs. In the second case, using a black-box approach, nonlinear system identification is still a challenging problem [7, 10, 11].

Roughly speaking, the PM approach consists of replacing this single, complex nonlinear model by a time-varying convex interpolation of a set of linear submodels. By appropriately choosing the number of submodels and the weighting functions, a large class of nonlinear models can be represented by a PM with a given prescribed precision. Therefore, the PMs are known to be universal approximators [2, 4–6, 8, 9, 13, 37, 38], and this mathematical representation offers an interesting way to avoid the specific analysis of the nonlinearities of the model, thanks to the specific PM properties. In this way, the PM approach reduces the complexity analysis, and makes it more practical for engineers.

PMs can be obtained from identification procedures (black-box modeling) or from transformations of a nonlinear model (white-box modeling). When input and output data of the system are available, black-box modeling is well adapted, and specific numerical optimization techniques for PM identification are proposed [9, 12, 13] to cope with the estimation of the submodels, as well as weighting function parameters, based on the optimization of a cost criterion. When a mathematical nonlinear model of the system is available, a white-box modeling procedure to obtain a PM can be followed. A simple way to obtain a PM form is based on

multiple linearizations using Taylor expansion of the nonlinear model around different operating points, and consequently the obtained PM is an approximation of the nonlinear model. Moreover, if the nonlinearities of the model are bounded, at least in a compact set, it is possible to rewrite a nonlinear model into a PM form [15, 33, 33]. In this way, the obtained PM is an exact rewriting of the nonlinear model, meaning that the state trajectories of both models are equal. In this section, this last approach is presented.

## 1.1 Polytopic Model Structure

Nonlinear dynamic deterministic systems can be represented using different forms of PMs, as summarized in [9, 26]; among them, the PM structure employed here is [3]

$$\dot{x}(t) = \sum_{i=1}^{r} \mu_i(\xi(t))\{A_i x(t) + B_i u(t)\} \tag{9.1a}$$

$$y(t) = \sum_{i=1}^{r} \mu_i(\xi(t)) C_i x(t) \tag{9.1b}$$

where $x \in \mathbb{R}^n$ is the state common to all submodels, $u \in \mathbb{R}^{n_u}$ is the control input, $y \in \mathbb{R}^{n_y}$ is the output, and $\mu_i(\cdot)$ are the weighting functions, depending on the premise variable $\xi(t) \in \mathbb{R}^{n_\xi}$.

The relative contribution of the $r$ submodels is quantified by the weighting functions $\mu_i(\cdot)$, which satisfy the convex sum constraints

$$0 \leq \mu_i(\xi) \leq 1, \quad \forall i = 1, \ldots, r \qquad \text{and} \qquad \sum_{i=1}^{r} \mu_i(\xi) = 1 \tag{9.2}$$

Defining the PM (9.1) with the weighting functions satisfying Eq. (9.2), the contribution of several submodels can be simultaneously taken into account with different weights over the range 0–1. Take note that the so-called premise variable $\xi(t)$ is used in order to take into account the current operating point of the system. It is here assumed that $\xi(t)$ is known and real-time accessible; currently the inputs and/or measured state variables are employed as premise variables.

PMs have been used for several years to cope with the modeling problem of systems subject to a finite number of operating modes. The main idea is to describe each mode with the help of a linear submodel, and then interpolate these submodels using the weighting functions $\mu_i$. Very similar mathematical forms of the PM structure (9.1) can be found in the literature, and several designations have been used, according to the theoretical modeling context, and the given interpretation of these weighting functions. For example, in the context of hybrid systems with finite

operation models, different approaches are investigated in the literature, such as piecewise affine (PWA) or switched systems [39–42], Markovian jump linear systems (MJLS) [43], and the MM [6, 18, 26, 28–30]. For PWA systems, the weighting functions $\mu_i$ take their values in the pair $\{0,1\}$; then only one submodel is taken into account at every time instant. For MJLS, the weighting functions $\mu_i$ represent transition probabilities given by a homogeneous Markov chain on a finite state space, as presented in [43]. PMs can also be built using the concept of the fuzzy sets theory and the weighting functions $\mu_i$ are fuzzy rules or membership functions employed as an inferred mechanism [3, 44]. A description of uncertain systems using the convex polytopic uncertainty can also be accomplished with the help of this mathematical structure [45]. The same mathematical representation is also employed in the quasi-linear parameter varying (q-LPV) systems theory to model some parameter variations, thanks to the weighting functions [1, 46].

## 1.2 How to Get a PM Using Nonlinear Sector Transformation?

The nonlinear sector transformation (NST) presented here, also known as the convex polytopic transformation, is certainly not an approximation of the original nonlinear system, but is an equivalent, and thus exact, rewriting of the original nonlinear model [15, 16, 33].

For the sake of clarity, the way to obtain a PM is illustrated with the help of a continuous-time scalar nonlinear model:

$$\dot{x}(t) = f(x(t),u(t))x(t) + g(x(t),u(t))u(t) \tag{9.3}$$

The following modeling assumption is the backbone of the sector transformation:

**Assumption 1.** The functions $f$ and $g$ are bounded, that is,

$$\underline{f} \le f(x,u) \le \overline{f}, \quad \underline{g} \le g(x,u) \le \overline{g}, \qquad \forall x,\ \forall u \tag{9.4}$$

for given distinct real numbers $\underline{f}, \overline{f}, \underline{g}$, and $\overline{g}$.

This assumption is always satisfied at least on a compact set of $x$ and $u$ for continuous derivable functions $f$ and $g$. It is important to emphasize that the obtained PM is only valuable in the operating region defined by Eq. (9.4). Consequently, all the stability properties presented in the following sections are only valid under Assumption 1; outside of the chosen compact set these properties are not guaranteed. Under Assumption 1, the functions $f$ and $g$ in Eq. (9.3) can be written as

$$f(x,u) = \mu_{11}(x,u)\underline{f} + \mu_{12}(x,u)\overline{f} \tag{9.5a}$$

$$g(x,u) = \mu_{21}(x,u)\underline{g} + \mu_{22}(x,u)\overline{g} \tag{9.5b}$$

where the weighting functions $\mu_{ij}(x,u)$ are

$$\mu_{11}(x,u) = \frac{\overline{f} - f(x,u)}{\overline{f} - \underline{f}} \quad \mu_{12}(x,u) = \frac{f(x,u) - \underline{f}}{\overline{f} - \underline{f}} \tag{9.6a}$$

$$\mu_{21}(x,u) = \frac{\overline{g} - g(x,u)}{\overline{g} - \underline{g}} \quad \mu_{22}(x,u) = \frac{g(x,u) - \underline{g}}{\overline{g} - \underline{g}} \tag{9.6b}$$

and satisfy the convex sum properties

$$\mu_{i1}(x,u) + \mu_{i2}(x,u) = 1, \quad 0 \le \mu_{ij}(x,u) \le 1, \qquad i,j = 1,2 \tag{9.7}$$

Consequently, the continuous-time scalar nonlinear model (9.3) can be written as

$$\dot{x}(t) = \sum_{i=1}^{2} \mu_{1i}(x,u) a_i x(t) + \sum_{j=1}^{2} \mu_{2j}(x,u) b_j u(t) \tag{9.8}$$

with $a_1 = \underline{f}$, $a_2 = \overline{f}$, $b_1 = \underline{g}$, and $b_2 = \overline{g}$. In order to have the same weighting functions in Eq. (9.8), the first (resp. second) sum of Eq. (9.8) can be multiplied by $\mu_{21} + \mu_{22} = 1$ (resp. $\mu_{11} + \mu_{12} = 1$), and thanks to the convex sum properties (9.7), the PM form (9.8) becomes

$$\dot{x}(t) = \sum_{i=1}^{4} \mu_i(x,u)\{A_i x(t) + B_i u(t)\} \tag{9.9}$$

that is clearly the same form as Eq. (9.1a), with the weighting functions $\mu_i(x,u)$

$$\mu_1(x,u) = \mu_{11}(x,u)\mu_{21}(x,u) \tag{9.10a}$$

$$\mu_2(x,u) = \mu_{11}(x,u)\mu_{22}(x,u) \tag{9.10b}$$

$$\mu_3(x,u) = \mu_{12}(x,u)\mu_{21}(x,u) \tag{9.10c}$$

$$\mu_4(x,u) = \mu_{12}(x,u)\mu_{22}(x,u) \tag{9.10d}$$

satisfying the convex sum properties (9.2), and with the submodel matrices defined by $A_1 = A_2 = \underline{f}$, $A_3 = A_4 = \overline{f}$, $B_1 = B_3 = \underline{g}$, and $B_2 = B_4 = \overline{g}$. The extension of this approach to vector differential equations with more than two nonlinearities is straightforward and can be found in [16].

It is important to mention that, if the nonlinearities of the functions $f$ and $g$ are not globally bounded on the state and input space, the PM (9.9) only provides the exact response of the nonlinear system (9.3) in the chosen compact set defined by Eq. (9.4), which often introduces bounds of $x$ and $u$. The state bound estimation for nonlinear systems according to the applied input $u(t)$ remains a difficult task because it depends on the control input, its dynamic, and those of the system. There are, however, some tractable approaches allowing one to enclose the reachable set of the

system states. In [47], the authors propose a $\mu$-formulation, which consists of transforming the state bounds estimation problem to a singularity problem. In [48], the problem is solved by computing an over-approximation of reachable sets. In [49], the proposed method uses additional physical information to improve enclosures with a minor additional cost. Outside this compact, the validity of the PM is not guaranteed, which constitutes the main limit of the presented modeling technique. Fortunately, in most real applications, the states are bounded, implying bounded nonlinearities, and Assumption 1 is then verified.

## 1.3 A Modeling Example

The polytopic modeling procedure is illustrated on a bioreactor model borrowed from Farza et al. [50]. The bioreactor consists of a microbial culture where a single biomass $X$ grows on a single substrate $P$, where the maintenance and decay processes are neglected. The process is described by the following nonlinear differential equations:

$$\dot{S}(t) = D(t)(S_{in}(t) - S(t)) - k\lambda \frac{S(t)}{K + S(t)} X(t) \tag{9.11a}$$

$$\dot{X}(t) = -D(t)X(t) + \lambda \frac{S(t)}{K + S(t)} X(t) \tag{9.11b}$$

where $D(t)$ is the known dilution rate, $S_{in}(t)$ is the input substrate concentration, and where the kinetic rate is given by a Monod's law parameterized by the maximum specific growth rate $\lambda$ and the saturation constant $K$. It is here assumed that the dilution rate is bounded by $D(t) \in \begin{bmatrix} D_{\min} & D_{\max} \end{bmatrix}$.

In order to turn the system (9.11) into a PM form using the NST, it is first rewritten as:

$$\begin{bmatrix} \dot{S}(t) \\ \dot{X}(t) \end{bmatrix} = \begin{bmatrix} -f(D(t)) & -k\lambda g(S(t)) \\ 0 & \lambda g(S(t)) - f(D(t)) \end{bmatrix} \begin{bmatrix} S(t) \\ X(t) \end{bmatrix} + \begin{bmatrix} f(D(t)) \\ 0 \end{bmatrix} S_{in}(t) \tag{9.12}$$

where the bounded system nonlinearities are defined by

$$f(D(t)) = D(t) \tag{9.13a}$$

$$g(S(t)) = \frac{S(t)}{K + S(t)} \tag{9.13b}$$

The dilution rate is bounded, then obviously so is $f(D(t)) = D(t)$. Moreover, the substrate concentration $S(t)$ is a positive growth, and so is the constant $K$; consequently the Monod's law $g(S(t)) \in \begin{bmatrix} 0 & 1 \end{bmatrix}$. Thus, the modeling Assumption 1 of bounded nonlinearities is satisfied

$$a_1 \leq f(D(t)) \leq a_2, \quad b_1 \leq g(S(t)) \leq b_2 \tag{9.14}$$

with $a_1 = D_{\min}$, $a_2 = D_{\max}$, $b_1 = 0$, and $b_2 = 1$ and the NST method can be applied. It is interesting to mention that, in this example, the nonlinearities

$f$ and $g$ are globally bounded. Consequently, the PM formulation of the nonlinear model is valid on the whole state and input spaces.

According to the foregoing, $f(D(t))$ and $g(S(t))$ can be expressed according to Eq. (9.5) using the functions $\mu_{ij}$ defined by Eq. (9.6), and the nonlinear model (9.11) can be rewritten as

$$\begin{bmatrix}\dot{S}(t)\\ \dot{X}(t)\end{bmatrix}=\begin{bmatrix}-\sum_{i=1}^{2}\mu_{1i}(D(t))a_i & -k\lambda\sum_{j=1}^{2}\mu_{2j}(S(t))b_j\\ 0 & \lambda\sum_{j=1}^{2}\mu_{2j}(S(t))b_j-\sum_{i=1}^{2}\mu_{1i}(D(t))a_i\end{bmatrix}\begin{bmatrix}S(t)\\ X(t)\end{bmatrix}+\begin{bmatrix}\sum_{i=1}^{2}\mu_{1i}(D(t))a_i\\ 0\end{bmatrix}S_{in}(t) \tag{9.15}$$

In Eq. (9.15), some terms depend on the weighting functions $\mu_{1i}$, while others depend on the functions $\mu_{2j}$. In order to have the PM form, a single summation using the same weighting functions should be obtained with the help of the convex sum property $\sum_{i=1}^{2}\mu_{ji}=1$ for $j=1,2$ as follows

$$\begin{bmatrix}\dot{S}(t)\\ \dot{X}(t)\end{bmatrix}=\sum_{j=1}^{2}\mu_{2j}(S(t))\sum_{i=1}^{2}\mu_{1i}(D(t))\left\{\begin{bmatrix}-a_i & -k\lambda b_j\\ 0 & \lambda b_j-a_i\end{bmatrix}\begin{bmatrix}S(t)\\ X(t)\end{bmatrix}+\begin{bmatrix}a_i\\ 0\end{bmatrix}S_{in}(t)\right\} \tag{9.16}$$

Finally, the nonlinear model (9.16) is rewritten into a PM form (9.1) by considering the following weighting functions

$$\mu_1(D(t),S(t))=\mu_{11}(D(t))\mu_{21}(S(t)) \tag{9.17a}$$
$$\mu_2(D(t),S(t))=\mu_{11}(D(t))\mu_{22}(S(t)) \tag{9.17b}$$
$$\mu_3(D(t),S(t))=\mu_{12}(D(t))\mu_{21}(S(t)) \tag{9.17c}$$
$$\mu_4(D(t),S(t))=\mu_{12}(D(t))\mu_{22}(S(t)) \tag{9.17d}$$

and the following submodel matrices

$$A_1=\begin{bmatrix}-a_1 & -k\lambda b_1\\ 0 & \lambda b_1-a_1\end{bmatrix}\qquad A_2=\begin{bmatrix}-a_1 & -k\lambda b_2\\ 0 & \lambda b_2-a_1\end{bmatrix}\qquad B_1=\begin{bmatrix}a_1\\ 0\end{bmatrix} \tag{9.18a}$$

$$A_3=\begin{bmatrix}-a_2 & -k\lambda b_1\\ 0 & \lambda b_1-a_2\end{bmatrix}\qquad A_4=\begin{bmatrix}-a_2 & -k\lambda b_2\\ 0 & \lambda b_2-a_2\end{bmatrix}\qquad B_3=\begin{bmatrix}a_2\\ 0\end{bmatrix} \tag{9.18b}$$

with $B_2=B_1$, $B_4=B_3$.

The simulations of the original nonlinear model (9.11), as well as the obtained PM, are shown in Fig. 9.2. The parameter values are the following: $k=3$, $\lambda=0.12$, $K=0.8$, $D_{\min}=0.3$, and $D_{\max}=0.45$. It can be seen that, under the considered assumptions, the state trajectories of the PM and of the nonlinear model are exactly the same, because the PM obtained using the NST is a rewriting of the nonlinear model, and not an approximation. This simple example clearly shows that the NST is an appropriate mathematical tool to transform a nonlinear model into a PM form in a compact sector.

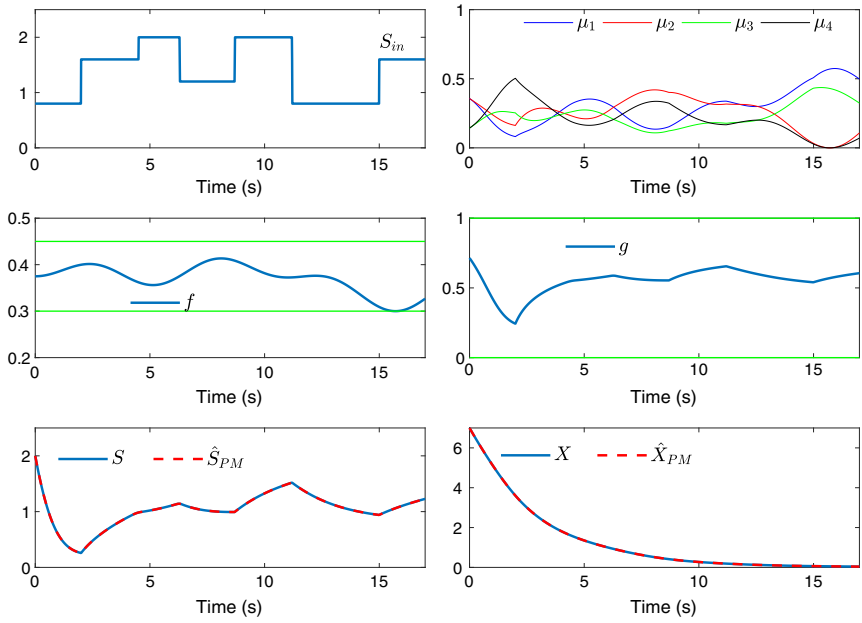


**FIG. 9.2** The bioreactor input $S_{in}(t)$ (*top left*) and the weighting functions $\mu_i(D(t), S(t))$, for $i = 1, \ldots, 4$ (*top right*). The nonlinear functions $f(D(t))$ (*middle left*) and $g(S(t))$ (*middle right*). The time evolutions of $S(t)$ (*bottom left*) and $X(t)$ (*bottom right*) obtained by simulating the original nonlinear model (*solid line*) and the PM (*dashed line*) are identical.

## 1.4 Partial Conclusion and Discussion

Some general remarks can be stated about the polytopic modeling approach. The PM obtained by the NST does not cause any loss of information from the original model in the considered compact set. All of the preceding results can be extended in a straightforward way to cope with the discrete-time case. In both cases, the number $r$ of submodels will increase with the number $q$ of nonlinearities considered following the polynomial rule $r = 2^q$. A large number of submodels increases the numerical burden of the stability conditions given in the next section.

Using the NST, the premise variables $\xi(t)$ in the weighting functions $\mu_i(\xi(t))$ depend on the same variables as the nonlinearities. Consequently, the premise variable $\xi(t)$ can be either real-time measured (e.g., $u$ or $y$), or unmeasured variables (e.g., $x$). In the previously considered example, the premise variable $\xi(t)$ was assumed to be real-time measurable. Of course, observer/controller design will be more difficult when $\xi(t)$ is an unmeasured variable. Solutions to cope with this problem are proposed in [25, 28–30, 33].

Notice that other PM structures can also be employed, such as the so-called decoupled or heterogeneous approach, where the PM is obtained

by blending the outputs of a set of LTI models [4, 6, 9]; but these approaches are out of the scope of this chapter. Finally, the PM order reduction can be performed using a descriptor approach, as proposed by Marx [51], in order to decrease the dimension of the state vector and design a controller of reasonable order for a complex process.

## 2 POLYTOPIC MODEL STABILITY

Analyzing the stability of nonlinear models is an important topic to design control laws, state observers, and so forth. However, even if several results are proposed in the literature, a systematic approach to cope with this problem is not available, because a specific analysis of the nonlinearities is often unavoidable [52]. Thanks to the PM approach, the stability analysis can be envisaged in a systematic way.

As previously mentioned, a PM provides an exact representation of a nonlinear model in an operating range. Consequently, the PM is nonlinear, and stability criteria established for linear systems, such as eigenvalue location, can no longer be applied. Furthermore, the stability of the linear submodels is not a sufficient condition for the stability of the PM. Indeed, the PM state trajectory depends on the weighting functions: the values of the weighting functions can cause instability, even if all the submodels are stable.

In order to illustrate this interesting stability result, an autonomous PM with two submodels is considered

$$\dot{x}(t) = \sum_{i=1}^{2} \mu_i(\xi(t)) A_i x(t), \quad x(0) \neq 0 \tag{9.19}$$

where the numerical values of matrices $A_i \in \mathbb{R}^{2\times 2}$ are inspired of [39, 40]

$$A_1 = \begin{bmatrix} -1 & 10 \\ -100 & -1 \end{bmatrix} \quad \text{and} \quad A_2 = \begin{bmatrix} -1 & 10 \\ -10 & -1 \end{bmatrix} \tag{9.20}$$

It is interesting to remark that the two considered submodels defined by $A_1$ and $A_2$ are stable, because their eigenvalues are, respectively, $-1 \pm \sqrt{1000}i$ and $-1 \pm 10i$. One should note that in [39, 40], switched systems are considered, and then only one submodel is taken into account at each instant-time. In the present example, however, the two submodels can be considered at each instant-time according to the weighting functions $\mu_i(\xi(t))$

$$\mu_i(\xi(t)) = \omega_i(\xi(t)) \Big/ \sum_{j=1}^{2} \omega_j(\xi(t)), \quad i = 1, 2 \tag{9.21a}$$

$$\omega_i(\xi(t)) = \exp(-(\xi(t) - c_i)^2/\sigma^2), \quad i = 1, 2 \tag{9.21b}$$

where $\xi(t)$ is the premise variable. The scalars $c_i$ and $\sigma$ are defined to shape the weighting functions in the operating space. Two different interpolations are studied. In the first case, the premise variable $\xi(t)$ is defined by

$$\xi(t) = x_1(t)x_2(t) \tag{9.22}$$

In the second one, $\xi(t)$ is given by

$$\xi(t) = -x_1(t)x_2(t) \tag{9.23}$$

In both cases, the scalars are the following: $c_1 = 0.15$, $c_2 = -0.15$, and $\sigma = 0.9$.

The phase trajectories of each stable submodel are shown in Fig. 9.3, considering the initial condition $x(0) = \begin{bmatrix}1 & 1\end{bmatrix}^T$. According to the premise variable choice, given by Eq. (9.22) or (9.23), a stable behavior is obtained in the first case, while an unstable behavior is obtained in the second one, as can be seen, respectively, on the bottom left and bottom right parts of Fig. 9.3.

This example shows that the stability of all individual submodels is not sufficient to draw a conclusion about the PM stability, because the interpolation of the submodels through the weighting functions affects

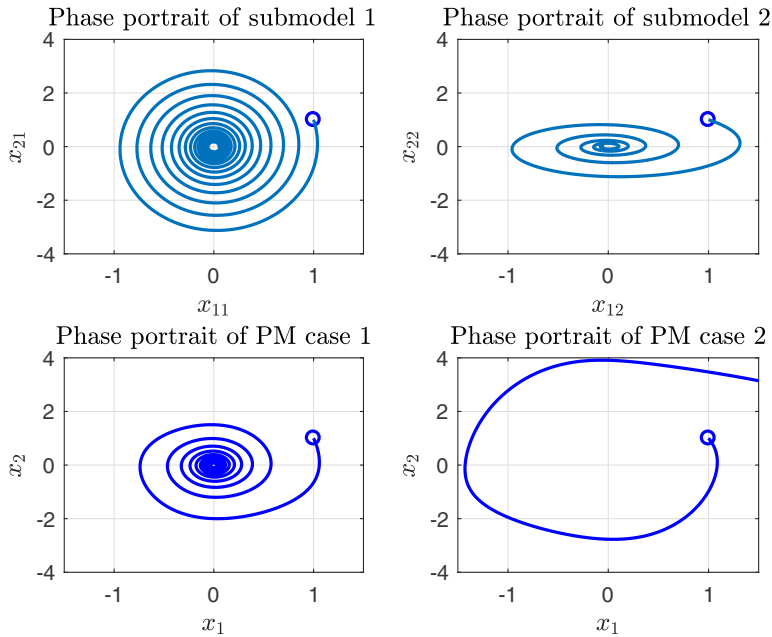


**FIG. 9.3** Examples of stability results for PMs. Phase portrait of the stable submodels $A_1$ and $A_2$ (*top left* and *right*). Phase portrait of the PM in the case 1 (*bottom left*) and in the case 2 (*bottom right*).

the PM stability. Thus appropriate stability tools must be proposed for PMs. Results for PM stability can be obtained from the Lyapunov's second method [52]. This method allows us to check the stability of nonlinear systems, without computing their state trajectory, by searching a so-called Lyapunov candidate function, depending on the state variables, that is nonnegative and decreasing.

In the PM framework, stability conditions based on the Lyapunov theory may be expressed as an LMI optimization problem. The conservatism level of the LMI problem to be numerically solved is mainly related to the choice of the candidate Lyapunov function, as well as the number and the dimension of the submodels. In this section, some LMI conditions ensuring the PM stability in a compact set for any blending of weighting functions are presented with the help of two kinds of candidate Lyapunov functions.

## 2.1 Analyzing the PM Asymptotic Stability

Let us illustrate the simplest procedure to obtain asymptotic stability conditions for an autonomous PM

$$\dot{x}(t) = \sum_{i=1}^{r} \mu_i(\xi(t)) A_i x(t), \quad x(0) \neq 0 \tag{9.24}$$

where the weighting functions $\mu_i$ satisfy the convex sum properties (9.2). First, the following quadratic candidate Lyapunov function is considered

$$V(x(t)) = x^T(t) P x(t) \quad P > 0 \quad P = P^T \tag{9.25}$$

Then, its time-derivative along the system trajectory (9.24) is given by

$$\dot{V}(x(t)) = x^T(t) \sum_{i=1}^{r} \mu_i(\xi(t)) \{A_i^T P + P A_i\} x(t) \tag{9.26}$$

Let us emphasize that even if the values of the weighting functions are not a priori available, thanks to the convex sum properties (9.2), the existence of a decreasing positive function $V$, ensuring asymptotic stability of Eq. (9.24) in the modeling compact set, reduces to finding a matrix $P$ satisfying the following set of LMIs

$$A_i^T P + P A_i < 0, \quad P = P^T > 0 \quad \text{for} \quad i = 1, \ldots, r \tag{9.27}$$

If a common Lyapunov matrix $P$, solution of the LMI set Eq. (9.27), can be found, it implies that the PM (9.24) is asymptotically stable. Nevertheless, because the LMI conditions (9.27) are only sufficient, it is not possible to draw conclusions about the (un)stability if no solution is found.

The main drawback of quadratic stability conditions (9.27) is that a single common matrix $P$ for all submodels must be obtained to conclude about the PM stability, increasing, in this way, the conservatism level of

the solution. This conservatism can be reduced by replacing the quadratic candidate Lyapunov function (9.25) by a parameter-dependent candidate Lyapunov function, such as [53]

$$V(x(t)) = x^T(t)P(\xi(t))x(t) \tag{9.28}$$

with

$$P(\xi(t)) = \sum_{i=1}^{r} \mu_i(\xi(t))P_i, \quad P_i > 0, \quad P_i = P_i^T \tag{9.29}$$

which generalizes the quadratic candidate Lyapunov function where $P_i = P$ is imposed. This Lyapunov function introduces some degree of freedom, thanks to the matrices $P_i$, and consequently the obtained stability results may be less conservative. Notice, however, that the time-derivative of $V(x(t))$ involves the time-derivative of the weighting functions

$$\dot{V}(x(t)) = x^T(t)\sum_{i=1}^{r} \dot{\mu}_i(\xi(t))P_i x(t) + x^T(t)\sum_{i=1}^{r} \mu_i(\xi(t))\{A_i^T P_i + P_i A_i\}x(t) \tag{9.30}$$

and upper bounds on the variation rate of the weighting functions must be computed. Based on the parameter-dependent candidate Lyapunov function (9.28), the following LMI stability condition is proposed in [53]

$$P_i + X \geq 0, \quad 1 \leq i \leq r \tag{9.31a}$$

$$\sum_{k=1}^{r} \phi_k(P_k + X) + \frac{1}{2}\{A_i^T P_j + P_j A_i + A_j^T P_i + P_i A_j\} < 0, \quad 1 \leq i \leq j \leq r \tag{9.31b}$$

where $X$ is a symmetric matrix, $P_i$ are positive definite symmetric matrices, and $\phi_k$ are the upper bound of the time derivative of the weighting functions: $|\dot{\mu}_k(\xi(t))| \leq \phi_k$. As illustrated in [53], the LMI conditions (9.31) allow the reduction of the conservatism. In the literature, the relaxation of the stability conditions is also investigated, based, for example, on some factorizations performed on the weighting functions [19–21], introducing additional slack variables [54, 55], and so forth. These last techniques are beyond the scope of this chapter, and in the sequel, for the sake of simplicity, only quadratic candidate Lyapunov functions will be employed.

## 2.2 Analyzing the PM Exponential Stability

The previous asymptotic stability conditions can be extended to investigate the exponential stability in order to guarantee a decay rate for the system state, which is of great importance to quantify dynamic performance in state feedback control and observer designs. Thanks to this decay rate, the convergence speed of the system state and/or

state estimation error can be imposed. As stated in [45], if the candidate Lyapunov function (9.25) satisfies

$$\dot{V}(x(t)) + 2\alpha V(x(t)) < 0 \tag{9.32}$$

then the decay rate, quantifying the convergence speed toward zero, is bounded by $\alpha > 0$. Namely the system state is bounded by

$$\|x(t)\| \leq \|x(0)\| \sqrt{\frac{\lambda_{\max}(P)}{\lambda_{\min}(P)}} e^{-\alpha t} \tag{9.33}$$

where $\lambda_{\min}(P)$ (resp. $\lambda_{\max}(P)$) denotes the minimum (resp. maximum) eigenvalue of $P$, and consequently, the convergence speed of $x$ toward zero is bounded by the value of the decay rate $\alpha$. By considering the inequality (9.32) instead of $\dot{V}(x(t)) < 0$ and following the previous developments, the asymptotic stability conditions (9.27) are replaced by

$$(A_i + \alpha I)^T P + P(A_i + \alpha I) < 0, \quad P = P^T > 0, \quad \alpha > 0, \quad \text{for } i = 1, \ldots, r \tag{9.34}$$

Maximizing the convergence speed by simultaneously seeking $P$ and the maximal $\alpha$ under constraints (9.34) gives rise to bilinear matrix inequalities (BMIs). A simple way to linearize the BMI problem (9.34) is to use an iterative dichotomic procedure, where at each step, $\alpha$ is fixed and $P$ is sought to solve the LMI. The procedure is stopped when the maximal $\alpha$ such that there exists a solution in $P$ is found. Notice also that specific solvers can be employed based, for example, on methods proposed in [56, 57].

It is interesting that the LMIs (9.27) for asymptotic stability and the BMIs (9.34) for exponential stability define particular regions of the complex plane. In fact, the LMIs (9.27) define the region given by the open left half-plane, while the BMIs (9.34) define the left half-plane delimited by $\Re(z) < -\alpha$. The definition of other regions of the complex plane using LMIs is also possible, and may introduce other dynamic specifications, such as, minimum damping ratio, as presented by Chilali et al. [58].

## 2.3 Analyzing the PM Stability With $\mathcal{L}_2$-Gain Performance

In many real-life cases, disturbances, such as noise, act on the system. These disturbances can be taken into consideration by considering the PM as

$$\dot{x}(t) = \sum_{i=1}^{r} \mu_i(\xi(t)) \{A_i x(t) + E_i d(t)\} \tag{9.35}$$

where $x(t) \in \mathbb{R}^n$ is the state, $d(t) \in \mathbb{R}^{n_d}$ is a disturbance signal with bounded $\mathcal{L}_2$-norm: $\|d\|_2^2 < \infty$ and where the weighting functions $\mu_i$ satisfy the convex sum properties (9.2).

The impact of $d(t)$ on the state is quantified by the $\mathcal{L}_2$-gain from $d(t)$ to $x(t)$, and the robust stability problem is then to keep the asymptotic stability of the PM when the disturbance is nil, and also to ensure

$$\|x\|_2^2 \leq \gamma^2 \|d\|_2^2 \quad \text{for } d(t) \neq 0 \text{ and } x(0) = 0 \tag{9.36}$$

where $\gamma > 0$ is the upper bound of the $\mathcal{L}_2$-gain from $d(t)$ to $x(t)$ to be minimized.

In order to maintain some dynamic performances, such as convergence speed toward zero, while ensuring robustness to disturbances, such as Eq. (9.36), one should seek to jointly obtain the *decay rate* $\alpha > 0$ of Eq. (9.33) and the attenuation level $\gamma > 0$ of Eq. (9.36). This stability problem can be tackled in a way that is similar to the previous stability problems by considering, for example, a quadratic Lyapunov function (9.25) satisfying the following condition [45]

$$\dot{V}(x(t)) < -2\alpha V(x(t)) - x^T(t)x(t) + \gamma^2 d^T(t)d(t) \tag{9.37}$$

Finally, the PM (9.35) satisfies the robust stability constraint (9.37) if the following conditions hold

$$\begin{bmatrix} P(A_i + \alpha I) + (A_i + \alpha I)^T P + I & PE_i \\ (PE_i)^T & -\gamma^2 \mathrm{I} \end{bmatrix} < 0, \quad i = 1, \ldots, r \tag{9.38}$$

for a matrix $P = P^T > 0$, a prescribed decay rate $\alpha > 0$ and an attenuation level $\gamma > 0$. Notice that Eq. (9.38) is an extension of the well-known bounded real lemma for LTI systems [45]. In several control or observer problem designs, the condition (9.38) is employed to simultaneously minimize the attenuation level $\gamma$ (by defining a new LMI variable $\bar{\gamma} = \gamma^2$) and maximize the decay rate $\alpha$. In this way, a trade-off between robustness and dynamic performances can be obtained.

## 2.4 Stability Analysis Example

The previous bioreactor example (9.11) can be considered again to illustrate the stability analysis of a PM. Using the LMI conditions (9.27), one can verify that the input-free system is globally quadratically stable. It is illustrated by the phase portrait displayed in Fig. 9.4, where initial conditions $(S(0), X(0)) \in \begin{bmatrix} 0 & 2.5 \end{bmatrix} \times \begin{bmatrix} 0 & 1.5 \end{bmatrix}$ were considered, and where it can be seen that $(S, X) = (0, 0)$ is an equilibrium point. Using Eq. (9.34), it can also be checked that the input-free PM is globally exponentially stable, with a maximum decay rate $\alpha = 0.855$.

## 2.5 Partial Conclusion and Discussion

In this section, the stability analysis of PM is presented with the use of the Lyapunov theory. Thanks to the PM formulation, the complexity of the problem is reduced because the specific analysis of the nonlinearities

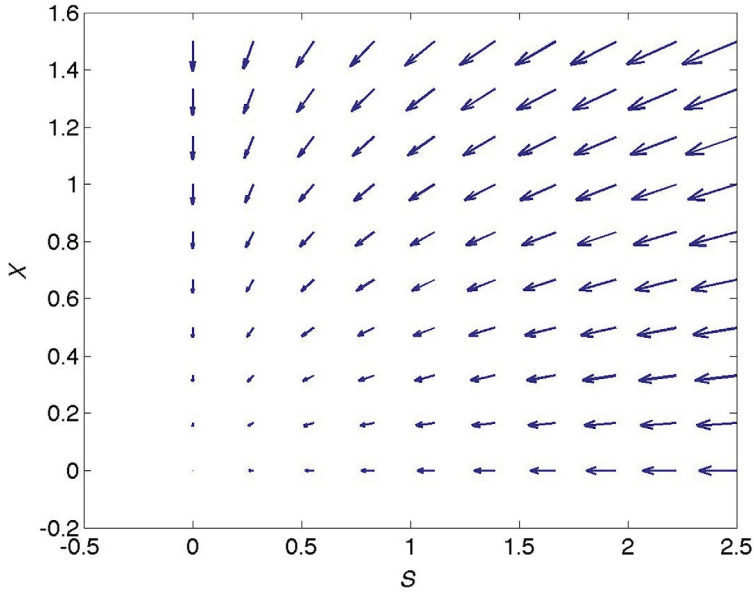


**FIG. 9.4** Phase portrait of the bioreactor example for $(S(0), X(0)) \in [0 \quad 2.5] \times [0 \quad 1.5]$.

is avoided. According to the chosen candidate, Lyapunov functions' sufficient stability conditions are given by a set of LMIs. If the obtained stability conditions are not under an LMI form, some techniques, such as state augmentation [59], or the descriptor approach [23, 60] may allow linearization of the BMIs, and also introduction of additional variables. Then the solution is provided by various software programs.

Note that the stability conditions are only sufficient because several Lyapunov functions could be employed, and it is not possible to draw conclusions about the (un)stability if no solution is found to the LMI problem. Consequently, a key topic in the PM stability analysis is the conservatism reduction which, despite active and ongoing research, remains an open problem.

One of the main goals of stability analysis is its extension to the controller and/or observer designs, as it will be shown in the next sections.

## 3 STATE FEEDBACK DESIGN BASED ON POLYTOPIC MODELS

In this section, stabilizing state feedback for nonlinear systems is investigated with the PM approach. The stability conditions previously presented can be employed for controller design, by ensuring the asymptotical convergence toward the origin and/or the robust stability of the closed-loop PM.

## 3.1 Classic State Feedback Design

Let us consider the PM (9.1a) with the static state feedback control law

$$u(t) = -Kx(t) \tag{9.39}$$

where the $K \in \mathbb{R}^{n_u \times n}$ is the state feedback gain to be found in order to ensure the stability of the following closed-loop system obtained from Eqs. (9.1a), (9.39)

$$\dot{x}(t) = \sum_{i=1}^{r} \mu_i(\xi(t))\{A_i - B_i K\}x(t) \tag{9.40}$$

Thanks to the established stability condition (9.34), the exponential stability with a decay rate $\alpha > 0$ is ensured for the closed-loop PM, if the following matrix inequalities hold

$$(A_i + \alpha I - B_i K)^T P + P(A_i + \alpha I - B_i K) < 0, \quad \alpha > 0, \quad \text{for } i = 1, \ldots, r \tag{9.41}$$

for a symmetric positive definite matrix $P \in \mathbb{R}^{n \times n}$. Let us remark that Eq. (9.41) is not an LMI because it involves the product of unknown parameters $P, K$, and $\alpha$. However, defining $Q = Q^T = P^{-1} > 0$ and $M = KQ$ and for a given $\alpha > 0$, Eq. (9.41) is equivalent to the following LMI in $Q$ and $M$

$$Q(A_i + \alpha I)^T + (A_i + \alpha I)Q - M^T B_i^T - B_i M < 0, \quad \text{for } i = 1, \ldots, r \tag{9.42}$$

and the state feedback gain is obtained by $K = MQ^{-1}$ for a given $\alpha > 0$.

## 3.2 Robust State Feedback Design With $\mathcal{L}_2$-Gain Performance

When a disturbance acts on the PM, it can be represented by

$$\dot{x}(t) = \sum_{i=1}^{r} \mu_i(\xi(t))\{A_i x(t) + B_i u(t) + E_i d(t)\} \tag{9.43}$$

where $x(t) \in \mathbb{R}^n$, $u(t) \in \mathbb{R}^{n_u}$, and $d(t) \in \mathbb{R}^{n_d}$ is a $\mathcal{L}_2$ bounded disturbance. The goal is to design a robust state feedback control law (9.39) such that the impact of the disturbance $d(t)$ on the state $x(t)$ is lowered by minimizing the attenuation level $\gamma > 0$ in Eq. (9.36). The disturbed closed-loop PM is then

$$\dot{x}(t) = \sum_{i=1}^{r} \mu_i(\xi(t))\{(A_i - B_i K)x(t) + E_i d(t)\} \tag{9.44}$$

The obtained PM is similar to Eq. (9.35), and the robust stability condition (9.38) can be employed to design the state feedback control by finding $P$ and $K$, satisfying the set of BMIs

$$\begin{bmatrix} P(A_i - B_iK + \alpha I) + (A_i - B_iK + \alpha I)^T P + I & PE_i \\ (PE_i)^T & -\gamma^2 \mathrm{I} \end{bmatrix} < 0, \quad i = 1, \ldots, r \tag{9.45}$$

for a matrix $P = P^T > 0$ and a given decay rate $\alpha > 0$. As previously mentioned, Eq. (9.45) is a BMI. Nevertheless, using the well-known Schur complement [45] and the variable change $M = KQ$, Eq. (9.45) can be equivalently rewritten as the following LMI

$$\begin{bmatrix} A_iQ + QA_i^T - B_iM - (B_iM)^T + 2\alpha Q + E_iE_i^T & Q \\ Q & -\gamma^2 \mathrm{I} \end{bmatrix} < 0, \quad i = 1, \ldots, r \tag{9.46}$$

where the state feedback gain is given by $K = MQ^{-1}$ for a prescribed decay rate $\alpha$ with a matrix $Q = Q^T > 0$. In this problem the attenuation level $\gamma$ must be minimized (by minimizing the LMI variable $\overline{\gamma} = \gamma^2$) to reduce the impact of $d(t)$ on the state $x(t)$, while $\alpha > 0$ should be maximized to introduce dynamic performances of the closed-loop.

## 3.3 Robust State Feedback Control Design: LMI Problem Programming and Simulation

The goal here is to design a robust state feedback control for the following disturbed nonlinear system

$$\dot{x}_1(t) = -0.2x_1(t) + x_2(t) + 0.2x_1^2(t)u(t) + 0.4d(t) \tag{9.47a}$$

$$\dot{x}_2(t) = -x_1(t) + 0.2\sin(x_1(t))x_2(t) + u(t) + 0.2d(t) \tag{9.47b}$$

According to the technique presented in the modeling section, the nonlinear system (9.47) can be exactly rewritten into a PM form, for $x_1 \in [-2.5 \quad 2.5]$, by applying the NST to the two following nonlinearities

$$f(x_1(t)) = \sin(x_1(t)) \tag{9.48a}$$

$$g(x_1(t)) = x_1^2(t) \tag{9.48b}$$

By considering $x_1 \in [-2.5 \quad 2.5]$, the nonlinear functions (9.48) are bounded by

$$a_1 \leq f(x_1(t)) \leq a_2, \quad b_1 \leq g(x_1(t)) \leq b_2 \tag{9.49}$$

with $a_1 = -1$, $a_2 = 1$, $b_1 = 0$, and $b_2 = 6.25$. Similarly to what was performed on the previous example, the nonlinear model (9.47) is rewritten into a PM (9.43) with the submodel matrices

$$A_1 = \begin{bmatrix} -0.2 & 1 \\ -1 & 0.2a_1 \end{bmatrix} A_3 = \begin{bmatrix} -0.2 & 1 \\ -1 & 0.2a_2 \end{bmatrix}$$

$$B_1 = \begin{bmatrix} 0.2b_1 \\ 1 \end{bmatrix} B_2 = \begin{bmatrix} 0.2b_2 \\ 1 \end{bmatrix} E_1 = \begin{bmatrix} 0.4 \\ 0.2 \end{bmatrix} \tag{9.50}$$

with $A_2 = A_1$, $A_4 = A_3$, $B_3 = B_1$, $B_4 = B_2$, $E_2 = E_1$, $E_3 = E_1$, and $E_4 = E_1$. The disturbance $d(t)$ acting on the system states is a pseudo-random noise drawn from the standard normal distribution. Two decay rates are considered, $\alpha = 0$ and $\alpha = 0.3$, corresponding to different dynamic specifications of the closed-loop response.

An example of programming the LMI problem (9.46) is given in Program 1. In this program, the PM matrices are defined, and thanks to the Yalmip interface [61], the LMIs are declared in a simple way. The set of LMIs is solved with Matlab coupled with the SeDuMi solver [62] to compute the state feedback gain $K$. The robust gain $K$ is computed considering a decay rate $\alpha$ and minimizing the attenuation level $\gamma = \sqrt{\overline{\gamma}}$. For $\alpha = 0$ the minimum attenuation level is $\overline{\gamma} = 0.58$, while the minimum admissible attenuation level is $\overline{\gamma} = 2.58$ for $\alpha = 0.3$. This example shows that the robustness and the dynamic performances objectives cannot simultaneously be satisfied, and a trade-off between them is necessary.

Fig. 9.5 shows the open-loop response, as well as the closed-loop ones obtained with the robust state feedback gain computed for each considered decay rate. The considered initial condition is $x(0) = \begin{bmatrix} 2 & -1 \end{bmatrix}^T$ which belongs the modeling compact set. As expected, it can be seen in Fig. 9.5 that the larger decay rate $\alpha = 0.3$ allows one to have a faster closed-loop response. The counterpart of this faster response is a loss of robustness to the disturbance and the requirement of higher values of $u(t)$, as illustrated in Fig. 9.6. Fig. 9.6 also shows the time evolution of the nonlinear function $g(t) = x_1^2(t)$, which remains bounded by Eq. (9.49).

## Program 1 MATLAB CODE SOURCE TO PROGRAM THE LMI PROBLEM (9.46)

```
% MATLAB example state feedback design
% submodel parameters
a1=-1;a2=1;b1=0;b2=6.25;beta=-0.2;
% submodel matrices
A1=[beta 1;-1 -beta*a1];A3=[beta 1;-1 -beta*a2];A2=A1;A4=A3;
B1=[-beta*b1;1];B2=[-beta*b2;1];B3=B1;B4=B2;
I=eye(2,2);%identity matrix definition
alpha=0.3%prescribed decay rate

Q = sdpvar(2,2,'symmetric');M = sdpvar(1,2,'full');%matrices to be found
gamma=sdpvar(1,1,'full'); % attenuation level to be minimized
LMI1=[A1*Q+Q*A1'-B1*M-(B1*M)'+2*alpha*Q+E1*E1' Q;Q' -gamma*I]
LMI2=[A2*Q+Q*A2'-B2*M-(B2*M)'+2*alpha*Q+E1*E1' Q;Q' -gamma*I]
LMI3=[A3*Q+Q*A3'-B3*M-(B3*M)'+2*alpha*Q+E1*E1' Q;Q' -gamma*I]
LMI4=[A4*Q+Q*A4'-B4*M-(B4*M)'+2*alpha*Q+E1*E1' Q;Q' -gamma*I]
F = [Q > 0.01*I, LMI1<0, LMI2<0, LMI3<0, LMI4<0];%LMI problem
solvesdp(F,gamma);
Qf = double(Q);Mf = double(M)
K=Mf*inv(Qf) %obtained state feedback gain
gamma=double(gamma) %obtained attenuation level
```

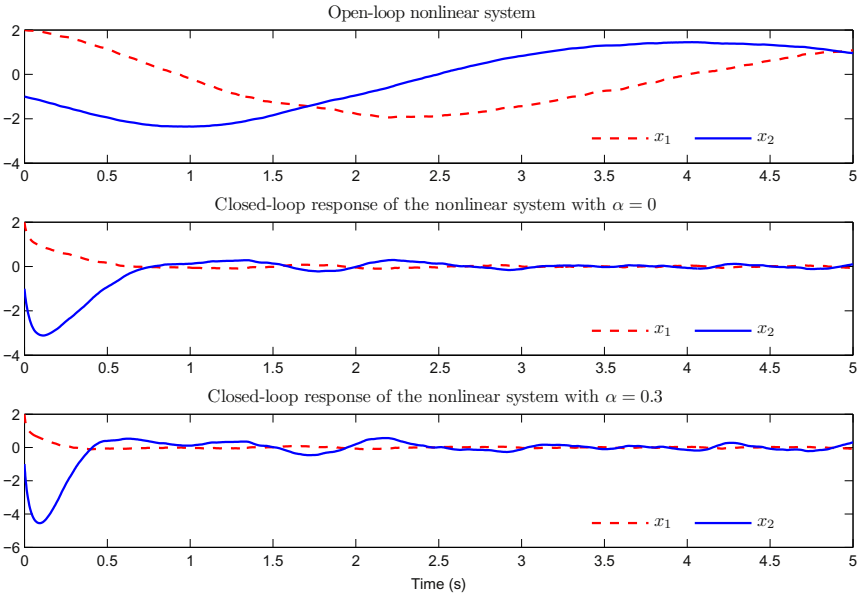


**FIG. 9.5** Robust state feedback control results. Open-loop response of the nonlinear system (*top*), closed-loop responses for the decay rate $\alpha = 0$ (*middle*), and for $\alpha = 0.3$ (*bottom*).

## 3.4 Partial Conclusion and Discussion

As seen in this section, even when disturbances act on the system, the stability conditions of the closed-loop system can be employed to design a state feedback controller by solving an LMI problem. Moreover, some desired closed-loop performances can be defined by specifying a minimum decay rate, or more generally, by ensuring the pole clustering of the closed-loop dynamics in some specific regions of the complex plane.

If the use of a common state feedback gain $K$ in the control law (9.39) increases the conservatism, then a solution to the LMI problem (9.42) or (9.46) may not be found. An interesting way to reduce this conservatism is to add some degree of freedom in the controller design by considering the following so-called parallel distributed compensation control law [17]

$$u(t) = -\sum_{i=1}^{r} \mu_i(\xi(t)) K_i x(t) \tag{9.51}$$

An intuitive way to see this control law structure is to consider that each submodel $(A_i, B_i)$ needs a different controller gain $K_i$ to be stabilized. In this case, the closed-loop PM is defined by a double sum

$$\dot{x}(t) = \sum_{i=1}^{r} \sum_{j=1}^{r} \mu_i(\xi(t)) \mu_j(\xi(t)) \{A_i - B_i K_j\} x(t) \tag{9.52}$$

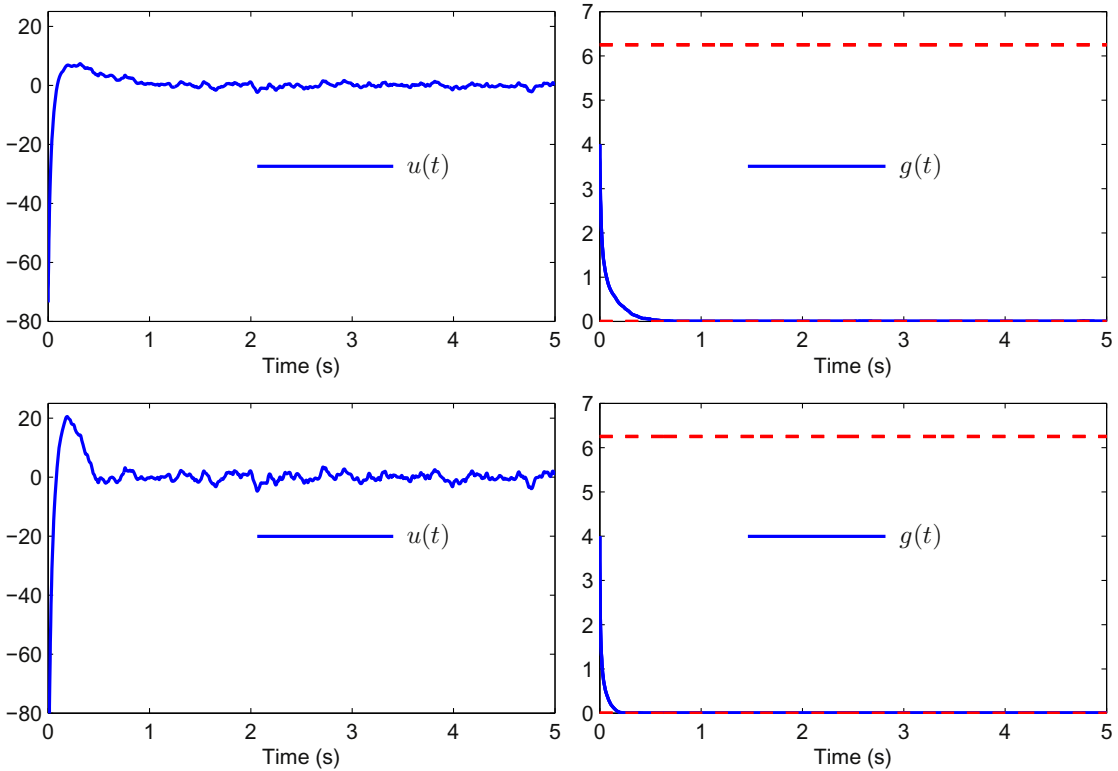


**FIG. 9.6** Time evolution of the input control $u(t)$ (*left*) and the nonlinear function $g(t) = x_1^2(t)$ (*right*) for $\alpha = 0$ (*top*) and for $\alpha = 0.2$ (*bottom*).

Studying the stability of Eq. (9.52) with a quadratic Lyapunov function (9.25) gives rise to BMI because of the coupling between the controller gains and the Lyapunov matrix $P$. Nevertheless, some variable changes, or the descriptor approach, allow one to obtain tractable LMI [17, 23].

# 4 OBSERVER STATE DESIGN BASED ON POLYTOPIC MODELS

In most cases, the whole system state vector is not measured due to economic or technological reasons. The lack of physical sensors to measure system states should be compensated by a virtual sensor, also known as state observers [63]. Based on a mathematical model of the system, the observer is designed in order that, fed with the known inputs and the measured outputs of the system, it provides a state estimate that converges toward the actual system state. This estimation must be provided in a large operating range of the nonlinear system, and for that, the PM approach is employed here.

## 4.1 Classic Proportional State Observer Design

First, the state observer design is presented considering the following PM

$$\dot{x}(t) = \sum_{i=1}^{r} \mu_i(\xi(t))\{A_i x(t) + B_i u(t)\} \tag{9.53a}$$

$$y(t) = Cx(t) \tag{9.53b}$$

with $x(t) \in \mathbb{R}^n$, $u(t) \in \mathbb{R}^{n_u}$, $y(t) \in \mathbb{R}^{n_y}$. The premise variable $\xi(t)$ is supposed to be real-time measurable. The polytopic proportional state observer can be defined as

$$\dot{\hat{x}}(t) = \sum_{i=1}^{r} \mu_i(\xi(t))\{A_i \hat{x}(t) + B_i u(t) + L_i(y(t) - \hat{y}(t))\} \tag{9.54a}$$

$$\hat{y}(t) = C\hat{x}(t) \tag{9.54b}$$

where the observer gains $L_i \in \mathbb{R}^{n \times n_y}$ must be found to ensure the convergence toward zero of the estimation error $e(t)$ defined by $e(t) = x(t) - \hat{x}(t)$, thanks to the proportional correction given by the observer gains $L_i$. From Eqs. (9.53), (9.54), the state estimation error dynamics can be expressed as

$$\dot{e}(t) = \sum_{i=1}^{r} \mu_i(\xi(t))\{A_i - L_i C\}e(t) \tag{9.55}$$

Similar to the previous controller design, the stability of Eq. (9.55) can be studied with a quadratic Lyapunov function (9.25). It leads us to establish the following LMI conditions of the convergence of $\hat{x}$ toward $x$

$$(A_i+\alpha I)^T P+P(A_i+\alpha I)-C^T N_i^T-N_i C<0, \quad \alpha>0, \quad \text{for } i=1,\ldots,r \tag{9.56}$$

with $P=P^T>0\in\mathbb{R}^{n\times n}$ and $N_i=PL_i\in\mathbb{R}^{n\times n_y}$. The observer gains are given by $L_i=P^{-1}N_i$ for a given decay rate $\alpha>0$.

## 4.2 Simultaneous Robust State and UI Estimation

In several situations, all the inputs acting on a system are not measurable, and thus some of them cannot be provided to the state observer. These unmeasurable inputs are often called UIs, and are often employed to model faults or neglected dynamics, and so forth. Let us now consider the PM with UI and disturbance

$$\dot{x}(t)=\sum_{i=1}^{r}\mu_i(\xi(t))\{A_i x(t)+B_i u(t)+E_i d(t)+F_i f(t)\} \tag{9.57a}$$

$$y(t)=Cx(t)+Gd(t)+Rf(t) \tag{9.57b}$$

where $x(t)\in\mathbb{R}^n$ is the state, $u(t)\in\mathbb{R}^{n_u}$ is the known input, $y(t)\in\mathbb{R}^{n_y}$ is the output, $d(t)\in\mathbb{R}^{n_d}$ is the disturbance, and $f(t)\in\mathbb{R}^{n_f}$ is the UI.

Here the main goals are, on one hand, not only to provide an estimation of the state, but also of the UI; and on the other hand, to minimize the disturbance impact on these estimations. The robust simultaneous estimation of the state and the UI of a system is a key problem in numerous automatic control problems [64, 65]. An effective way to obtain the simultaneous state and UI estimation is provided by the proportional-integral observer (PIO). A PIO is an extension of the proportional state observer (well known as Luenberger observer) employed to simultaneously compute state and UI estimations [52, 66]. The PIO can provide the UI estimate under the two following assumptions

**Assumption 2.** The UI signal $f(t)$ is a constant signal.

**Assumption 3.** The disturbance is a $\mathcal{L}_2$-bounded signal with $\|d\|_2^2<\infty$.

The proposed polytopic PIO structure is given by [27]

$$\dot{\hat{x}}(t)=\sum_{i=1}^{r}\mu_i(\xi(t))\{A_i\hat{x}(t)+B_i u(t)+F_i\hat{f}(t)+L_i(y(t)-\hat{y}(t))\} \tag{9.58a}$$

$$\dot{\hat{f}}(t)=\sum_{i=1}^{r}\mu_i(\xi(t))\tilde{L}_i(y(t)-\hat{y}(t)) \tag{9.58b}$$

$$\hat{y}(t)=C\hat{x}(t)+R\hat{f}(t) \tag{9.58c}$$

where $\hat{x}(t)\in\mathbb{R}^n$ is the estimated state and $\hat{f}(t)\in\mathbb{R}^{n_f}$ the estimate of the UI $f(t)$. The matrices $L_i\in\mathbb{R}^{n\times n_y}$ and $\tilde{L}_i\in\mathbb{R}^{n_f\times n_y}$ are the observer gains to be designed. The integral action of the PIO, introduced by Eq. (9.58b),

can be considered as a state augmentation, allowing estimation of not only the system state, but also the UI. The robustness properties of the PIO are investigated in [52, 66], and the PIO has been successfully employed in order to cope with state and UI estimation [67–69].

The PIO existence conditions are obtained by considering the dynamics of the state and UI estimation errors, respectively, denoted as $e(t)$ and $e_f(t)$, and defined by

$$e(t) = x(t) - \hat{x}(t), \quad e_f(t) = f(t) - \hat{f}(t) \tag{9.59}$$

Using Eqs. (9.57)–(9.59), the time-derivative of the estimation errors are then given by

$$\dot{\bar{e}}(t) = \sum_{i=1}^{r} \mu_i(\xi(t))\{(\bar{A}_i - \bar{L}_i\bar{C})\bar{e}(t) + (\bar{E}_i - \bar{L}_iG)d(t)\} \tag{9.60}$$

where

$$\bar{e}(t) = \begin{bmatrix} e(t) \\ e_f(t) \end{bmatrix}, \quad \bar{A}_i = \begin{bmatrix} A_i & F_i \\ 0 & 0 \end{bmatrix}, \quad \bar{L}_i = \begin{bmatrix} L_i \\ \tilde{L}_i \end{bmatrix}, \quad \bar{C} = \begin{bmatrix} C^T \\ R^T \end{bmatrix}^T, \quad \bar{E}_i = \begin{bmatrix} E_i \\ 0 \end{bmatrix} \tag{9.61}$$

The robust PIO design problem can thus be formulated as finding the augmented matrices $\bar{L}_i$ such that the estimation error $\bar{e}(t)$ vanishes to zero when no disturbances affect the system, and such that the influence of $d(t)$ on $\bar{e}(t)$ is minimized. This influence is quantified by the $\mathcal{L}_2$-gain from $d(t)$ to $\bar{e}(t)$.

The robust PIO design turns into finding $\bar{L}_i$ such that

$$\lim_{t\to\infty} \bar{e}(t) = 0 \quad \text{for} \quad d(t) = 0 \tag{9.62a}$$

$$\|\bar{e}\|_2^2 \leq \gamma^2 \|d\|_2^2 \quad \text{for} \quad d(t) \neq 0 \text{ and } \bar{e}(0) = 0 \tag{9.62b}$$

where $\gamma > 0$ is the upper bound of the $\mathcal{L}_2$-gain from $d(t)$ to $\bar{e}(t)$ to be minimized. Condition (9.62a) ensures the state estimate convergence toward the state variable despite the UI $f(t)$. This condition will be satisfied by imposing the exponential convergence of the estimation error to ensure a minimum *decay rate*, and thus to improve dynamic performances of the PIO. Condition (9.62b) ensures the disturbance attenuation on the state estimation. The PIO observer design can be tackled similarly to the previous robust stabilization problem.

Finally, the PIO (9.58) based on the PM (9.57), under constraints (9.62), is obtained if there exists a symmetric, positive definite matrix $P$ and matrices $M_i$ (for $i = 1, \ldots, r$) minimizing $\overline{\gamma} > 0$ under the LMIs for a prescribed $\alpha > 0$

$$\begin{bmatrix} \Delta_i + \Delta_i^T + I & P\bar{E}_i - M_iG \\ (P\bar{E}_i - M_iG)^T & -\overline{\gamma}\, \mathrm{I} \end{bmatrix} < 0, \quad i = 1, \ldots, r \tag{9.63}$$

where $\Delta_i = P(\bar{A}_i + \alpha \mathrm{I}) - M_i \bar{C}$. The observer gains are given by $\bar{L}_i = P^{-1} M_i$ and the upper bound of the $\mathcal{L}_2$-gain from $d(t)$ to $\bar{e}(t)$ is given by $\gamma = \sqrt{\overline{\gamma}}$.

## 4.3 PIO Design and Simulation

The goal here is to illustrate the joint state and UI estimation for the nonlinear system (9.47) using a PIO. For that purpose, it is assumed that $x_1(t)$ is the only measured state and $x_2(t)$ should be estimated. The input $u(t)$ of the system is affected by a piecewise constant UI, such as an actuator fault $f(t)$, to be estimated. On the other hand, an additive noise $d(t)$ acts on the output, as represented in Fig. 9.7.

The PM (9.57) is then defined by the matrices (9.50), $E_i = 0$, $F_i = B_i$, $C = \begin{bmatrix} 1 & 0 \end{bmatrix}$, $G = 0.4$, and $R = 0$. The noise is a pseudo-random noise drawn from the standard normal distribution.

For the PIO design, a trade-off between convergence speed of estimation errors and robustness of the estimation to the disturbance is obtained using the following parameters $\alpha = 0.1$, $\overline{\gamma} = 0.4$. The observer gains $\bar{L}_i$ obtained by solving the LMI problem (9.63) are

$$\bar{L}_1 = \begin{bmatrix} 13.02 \\ 16.30 \\ 11.60 \end{bmatrix}, \quad \bar{L}_2 = \begin{bmatrix} 24.61 \\ 31.21 \\ 23.67 \end{bmatrix}, \quad \bar{L}_3 = \begin{bmatrix} 10.55 \\ 12.94 \\ 9.27 \end{bmatrix}, \quad \bar{L}_4 = \begin{bmatrix} 22.23 \\ 27.97 \\ 21.42 \end{bmatrix} \tag{9.64}$$

The estimation results provided by the designed PIO are shown in Fig. 9.8. Notice that the initial condition of the system is $x(0) = \begin{bmatrix} 2 & -1.8 \end{bmatrix}^T$, while the one of the PIO is zero. These figures show the performances of

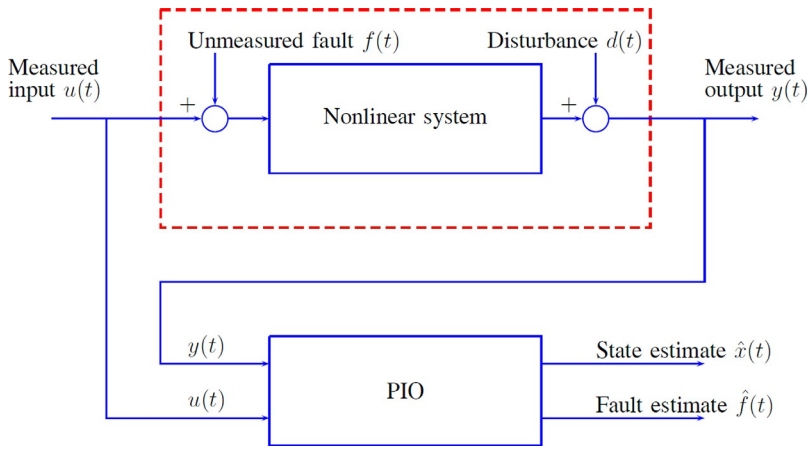


**FIG. 9.7** System and proportional-integral observer interconnection considered in the example.

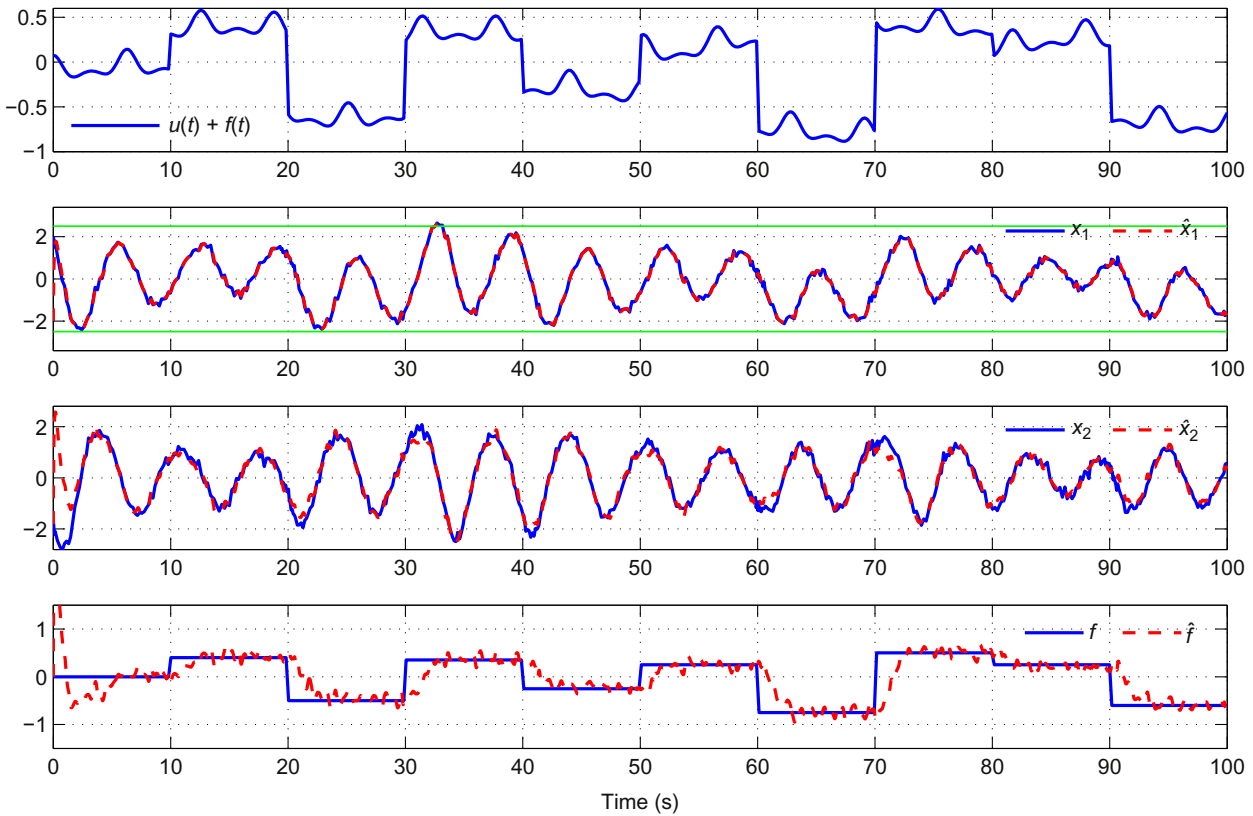


**FIG. 9.8** Estimation results provided by the proportional-integral observer. The faulty input signal $u(t) + f(t)$ is plotted on the *top*, the state $x(t)$ and their estimates $\hat{x}(t)$ in the *middle*, and $f(t)$ and $\hat{f}(t)$ at the *bottom*.

the joint state and actuator fault estimations, even when a noise acts on the output.

## 4.4 Partial Conclusion and Discussion

In this section, observer designs are presented to provide nonlinear state estimation, as well as UI estimation in a large operating range. The first observer, namely the proportional observer, only provides the system state estimate. The presented LMI condition (9.56) can easily be modified to handle a disturbance acting on a system. The second observer (PIO) generalizes the first one, because simultaneous estimation of the state and the UI is possible. Here, the considered UI is constant, or has small time variations $\dot{f}(t) \approx 0$. Improvements to the given PIO, in order to take into consideration a more general class of UI, for example, a polynomial form with respect to time $f(t) = a_0 + a_1 t + a_2 t^2 + \cdots + a_n t^n$, can be obtained following a similar approach using a proportional multiintegral observer with $(n + 1)$ integral terms in the dynamic equation of the observer, as presented in [27].

When the UI is considered a fault, the PIO can be used to provide fault detection, isolation, and estimation of faults acting on the system. The fault estimate can also be used online in the control law design to counteract the fault effect on the system trajectory. This is the aim of the FTC detailed in the next section.

# 5 ACTIVE FAULT-TOLERANT CONTROL

Several approaches have been developed in recent years in the framework of FTC design, which can be classified into two categories: passive FTC and active FTC [70, 71]. Even if FTC for linear systems have been intensively treated [72–74], FTC for nonlinear systems remains a challenging problem, and the PM approach is a promising way to tackle it.

In the previous sections, results related to modeling, stability analysis, state feedback design, and state observers with UI estimation design were presented using PM. This section shows how these results can be combined in an interesting way to cope with the FTC of nonlinear systems. The state feedback controller and the PIO providing state and UI estimation can be combined into an unified active fault-tolerant controller architecture. The term *active* means that the control signal is automatically reconfigured when a fault occurs, thanks to the fault detection identification and estimation (FDIE) provided by the PIO. The FDIE information, such as the time of occurrence of a fault (detection), fault location (isolation), and fault magnitude (estimation), are taken into account in the controller design to generate a control signal that preserves the system stability and performance.

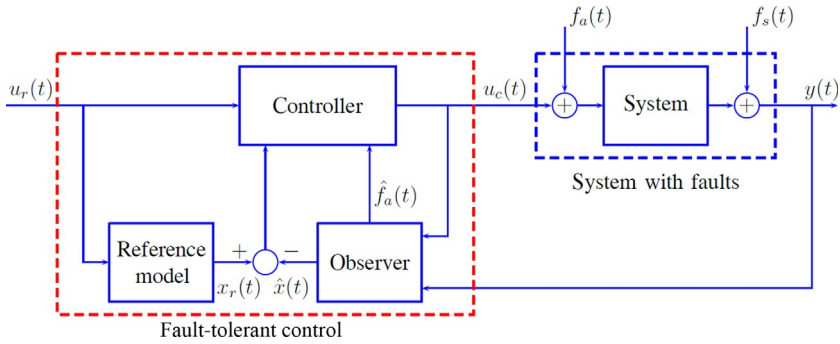


**FIG. 9.9** Fault-tolerant controller architecture.

The design of the FTC proposed here is based on the PM representation

$$\dot{x}(t) = \sum_{i=1}^{r} \mu_i(\xi(t))\{A_i x(t) + B_i(u_c(t) + f_a(t))\} \tag{9.65a}$$

$$y(t) = Cx(t) + Rf_s(t) \tag{9.65b}$$

where $x(t) \in \mathbb{R}^n$, $u_c(t) \in \mathbb{R}^{n_u}$, $y(t) \in \mathbb{R}^{n_y}$, $f_a(t) \in \mathbb{R}^{n_u}$, and $f_s(t) \in \mathbb{R}^{n_y}$. The faults $f_a(t)$ and $f_s(t)$, respectively, act on the actuators and the sensors. These faults can be considered UIs acting on the system, and they are here assumed to be constant.

As depicted in Fig. 9.9, the investigated FTC uses the state and UI estimates provided by the previously studied PIO to build the control input $u_c(t)$ (Eq. 9.67e) applied to the controlled system. The control law is then designed to perform reference state tracking, that is, in order to minimize the system state trajectory deviation caused by the faults using the robust stability condition. The state trajectory deviation is defined with regard to a reference state trajectory $x_r(t)$, provided by the following fault-free reference PM

$$\dot{x}_r(t) = \sum_{i=1}^{r} \mu_i(\xi(t))\{A_i x_r(t) + B_i u_r(t)\} \tag{9.66}$$

fed with the reference input $u_r(t)$ and where $x_r(t)$ is the state of the nominal (healthy) fault-free PM.

The active FTC, depicted in Fig. 9.9, is written as

$$\dot{\hat{x}}(t) = \sum_{i=1}^{r} \mu_i(\xi(t))\{A_i\hat{x}(t) + B_i(u_c(t) + \hat{f}_a(t)) + L_i(y(t) - \hat{y}(t))\} \tag{9.67a}$$

$$\hat{y}(t) = C\hat{x}(t) + R\hat{f}_s(t) \tag{9.67b}$$

$$\dot{\hat{f}}_a(t) = \sum_{i=1}^{r} \mu_i(\xi(t))H_i^a(y(t) - \hat{y}(t)) \tag{9.67c}$$

$$\dot{\hat{f}}_s(t) = \sum_{i=1}^{r} \mu_i(\xi(t)) H_i^s (y(t) - \hat{y}(t)) \tag{9.67d}$$

$$u_c(t) = -\sum_{i=1}^{r} \mu_i(\xi(t)) K_i(\hat{x}(t) - x_r(t)) - \hat{f}_a(t) + u_r(t) \tag{9.67e}$$

Eqs. (9.67a), (9.67b) are related to the state estimation of the system, and it is noteworthy that the fault estimates $\hat{f}_a(t)$ and $\hat{f}_s(t)$ are employed to improve the state estimation. The fault estimations $\hat{f}_a(t)$ and $\hat{f}_s(t)$ are obtained using the same strategy as employed by the PIO already presented with the help of Eqs. (9.67c), (9.67d).

The goal of the FTC (9.67) is to ensure reference state tracking, such that the faulty system state $x$ converges toward the reference state $x_r$ even when faults act on the system. For that purpose, the following tracking and estimation errors are defined

$$e_x(t) = x(t) - x_r(t), \quad \bar{e}(t) = \begin{bmatrix} x(t) - \hat{x}(t) \\ f_a(t) - \hat{f}_a(t) \\ f_s(t) - \hat{f}_s(t) \end{bmatrix} \tag{9.68}$$

where $e_x(t)$ is the tracking error between the system state and the reference model state. Because constant faults are considered, the closed-loop system can be written as the autonomous PM

$$\begin{bmatrix} \dot{\bar{e}}(t) \\ \dot{e}_x(t) \end{bmatrix} = \sum_{i=1}^{r} \mu_i \begin{bmatrix} \bar{A}_i - \bar{L}_i \bar{C} & 0 \\ \begin{bmatrix} B_i K_j & B_i & 0 \end{bmatrix} & A_i - B_i K_j \end{bmatrix} \begin{bmatrix} \bar{e}(t) \\ e_x(t) \end{bmatrix} \tag{9.69}$$

where the matrices $\bar{A}_i$, $\bar{L}_i$, and $\bar{C}$ are

$$\bar{A}_i = \begin{bmatrix} A_i & B_i & 0 \\ 0 & 0 & 0 \\ 0 & 0 & 0 \end{bmatrix}, \quad \bar{L}_i = \begin{bmatrix} L_i \\ H_i^a \\ H_i^s \end{bmatrix}, \quad \bar{C} = \begin{bmatrix} C^T \\ 0 \\ R^T \end{bmatrix}^T \tag{9.70}$$

Then the active FTC design problem can be formalized as finding the gains $L_i$, $H_i^a$, $H_i^s$, and $K_i$ such that the autonomous closed-loop system (9.69) is stable.

The stability of the autonomous PM (9.69) can be investigated with the help of a quadratic Lyapunov function, following the same steps as in the proof of Theorem 1 of [29] and using the relaxation scheme proposed in [20]. Finally, the FTC design reduces to find matrices $Q = Q^T > 0$, $P_1 = P_1^T > 0$, $X_2 = X_2^T > 0$, $\bar{K}_i$, and $\bar{Z}_i$ satisfying the following sufficient LMI conditions for a given positive $\lambda > 0$

$$\begin{cases} \Xi_{ii} < 0 & i = 1, \ldots, r \\ \frac{1}{r-1} \Xi_{ii} + \Xi_{ij} + \Xi_{ji} < 0 & i < j \end{cases} \tag{9.71}$$

where the symmetric matrix $\Xi_{ij}$ is defined by

$$\Xi_{ij} = \begin{bmatrix} -2\lambda \mathrm{diag}(Q, X_2, I_{n_y}) & * & * \\ \begin{bmatrix} B_i\bar{K}_j & B_iX_2 & 0 \end{bmatrix} & \mathrm{He}(A_iQ - B_i\bar{K}_j) & * \\ \lambda I_{n+n_u+n_y} & 0 & \mathrm{He}(P_1\bar{A}_i - Z_iC) \end{bmatrix} \quad (9.72)$$

where $\mathrm{diag}(Q, X_2, I_{n_y})$ denotes a block diagonal matrix with $Q$, $X_2$, and $I_{n_y}$ on its diagonal entries and where $\mathrm{He}(X) = X + X^T$, for any square matrix $X$. Finally, after solving Eq. (9.71), the observer and controller gains are obtained from

$$\begin{bmatrix} L_i^T & (H_i^a)^T & (H_i^s)^T \end{bmatrix}^T = P_1^{-1}Z_i, \quad K_i = \bar{K}_iQ^{-1}, \quad i = 1, \ldots, r \quad (9.73)$$

## 5.1 FTC Applied to Vehicle Lateral Dynamics

The FTC (9.67) is applied to ensure the lateral dynamic stability of a vehicle. In hard driving maneuvers, the vehicle lateral stability may be lost, then the vehicle spins and the driver loses control. In these critical situations, appropriate automatic corrective actions to maintain vehicle stability can be generated using specific control strategies. Here, the purpose of the FTC strategy is to provide a stabilizing yaw moment at the center of gravity (CoG) of the vehicle to keep the vehicle stable even when faults act on the vehicle, as depicted in Fig. 9.10. The PM approach is here applied to design

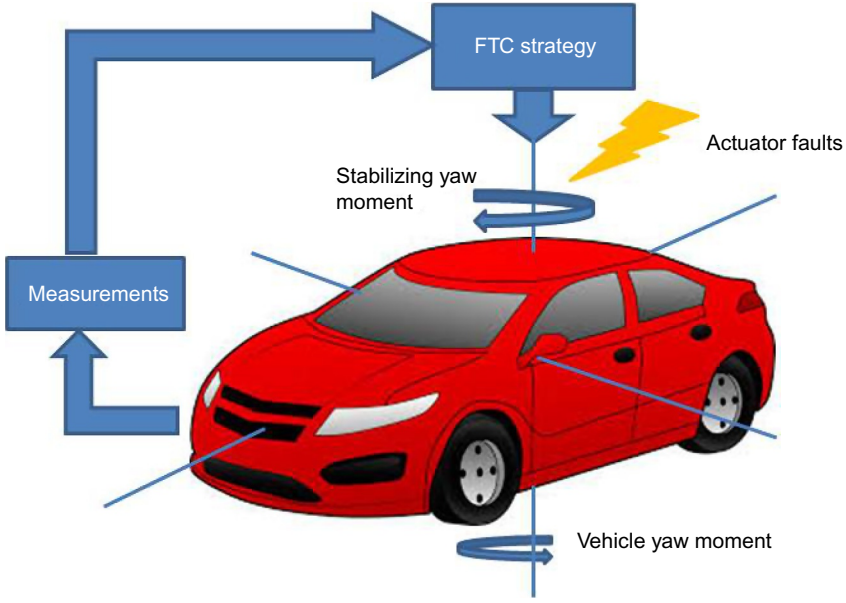


**FIG. 9.10** Fault-tolerant control for vehicle lateral stability.

an FTC strategy in the whole vehicle operating range, and in particular for different longitudinal velocities.

The FTC strategy is based on the single-track vehicle model that is a simplified dynamic model for the lateral vehicle motion [75]. The lateral position $y$ and the vehicle yaw angle $\psi$ are the two degrees of freedom of this model, as depicted in Fig. 9.11. This model is obtained by applying Newton's second law of motion, and by considering some assumptions, such as, nonroad bank angle, and the same steering angle for both front wheels and lateral tire forces in their linear region. Finally, the state space nonlinear model of the single-track vehicle is [75]

$$\begin{bmatrix} \dot{v}_y(t) \\ \ddot{\psi}(t) \end{bmatrix} = \begin{bmatrix} -\frac{C_f+C_r}{mv_x(t)} & -\frac{a_fC_f-a_rC_r}{mv_x(t)} - v_x(t) \\ -\frac{a_fC_f-a_rC_r}{I_zv_x(t)} & -\frac{a_f^2C_f+a_r^2C_r}{I_zv_x(t)} \end{bmatrix} \begin{bmatrix} v_y(t) \\ \dot{\psi}(t) \end{bmatrix} \tag{9.74a}$$

$$+ \begin{bmatrix} \frac{C_f}{m} \\ \frac{a_fC_f}{I_z} \end{bmatrix} \delta_f(t) + \begin{bmatrix} 0 \\ \frac{1}{I_z} \end{bmatrix} M_z(t) \tag{9.74b}$$

$$y(t) = \begin{bmatrix} 0 & 1 \end{bmatrix} \begin{bmatrix} v_y(t) & \dot{\psi}(t) \end{bmatrix}^T \tag{9.74c}$$

where $v_y(t)$ and $\dot{\psi}(t)$, respectively, denote the lateral velocity and the yaw rate. The driver acts on the vehicle through the steering angle $\delta_f(t)$ considered as a measured input that is not computed by the FTC controller, but may be provided to it. In fact, the controlled input to stabilize the vehicle yaw motion is the stabilizing yaw moment $M_z(t)$ generated by a differential braking on the rear wheels. The measured output is the yaw

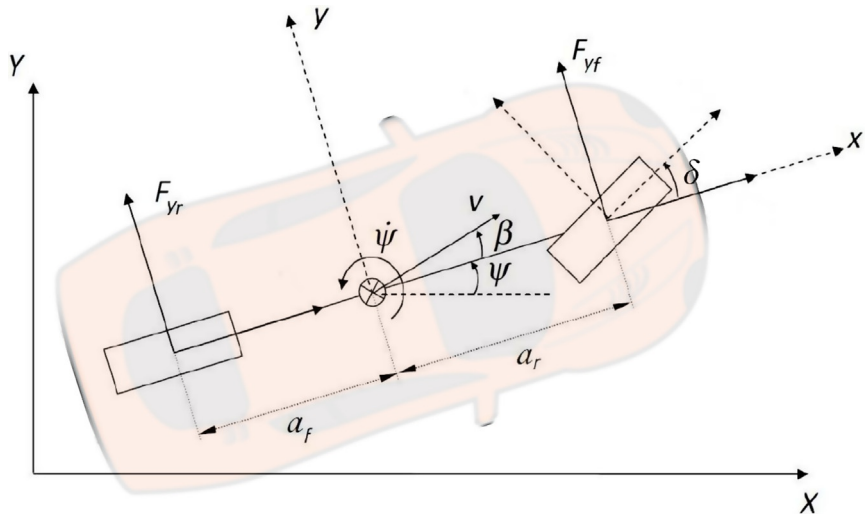


**FIG. 9.11** Single-track model.

**TABLE 9.1** Variables and Parameters of the Single-Track Vehicle Model

| | |
|---|---|
| **TIME-VARYING VARIABLES** | |
| $\dot{\psi}$ | Yaw rate |
| $v_x, v_y$ | Longitudinal and lateral velocities |
| **CONSTANT PARAMETERS** | |
| $m = 1700$ kg, $I_z = 2454$ kg m$^2$ | Vehicle mass and inertia |
| $a_f = 1.1$ m, $a_r = 1.44$ m | Distances from the front and rear axle to the CoG |
| $C_f = 61{,}000$ N/rad, $C_r = 48{,}000$ N/rad | Stiffness coefficients of the front and rear tires |

rate $\dot{\psi}(t)$, which is provided by the inertial unit. The estimation of the lateral velocity is then needed to use a state feedback control. It can be noted that the longitudinal velocity $v_x(t)$, measured in real-time, is time-varying, and consequently the model (9.74) is nonlinear. All variables and parameters used in this model are summarized in Table 9.1.

The first goal is to obtain a PM representation of the single-track vehicle model (9.74). From Eq. (9.74b), two time-varying terms $v_x(t)$ and $1/v_x(t)$ are considered, and the premise variable is the longitudinal velocity $v_x(t) \neq 0$. Because the longitudinal velocity is bounded by $\underline{v_x} \leq v_x(t) \leq \overline{v_x}$, then the two nonlinearities $f$ and $g$ defined by $f(v_x(t)) = v_x(t)$ and $g(v_x(t)) = 1/v_x(t)$ are also bounded: $\underline{f} \leq f(v_x(t)) \leq \overline{f}$ and $\underline{g} \leq g(v_x(t)) \leq \overline{g}$. Applying the NST, see Eqs. (9.5), (9.6), to $f(v_x(t))$ and $g(v_x(t))$, the following fault-free PM is obtained

$$\dot{x}(t) = \sum_{i=1}^{4} \mu_i(v_x(t))\{A_i x(t) + BM_z(t) + E\delta_f(t)\} \tag{9.75a}$$

$$y(t) = Cx(t) \tag{9.75b}$$

The state is defined by $x(t) = \begin{bmatrix} v_y(t) & \dot{\psi}(t) \end{bmatrix}^T$, $M_z(t)$ is the control input, and the matrices of the four submodels are

$$A_1 = \begin{bmatrix} \beta_{11}\underline{f} & \beta_{12}\underline{f} - \underline{g} \\ \beta_{21}\underline{f} & \beta_{22}\underline{f} \end{bmatrix}, \quad A_2 = \begin{bmatrix} \beta_{11}\underline{f} & \beta_{12}\underline{f} - \overline{g} \\ \beta_{21}\underline{f} & \beta_{22}\underline{f} \end{bmatrix} \tag{9.76a}$$

$$A_3 = \begin{bmatrix} \beta_{11}\overline{f} & \beta_{12}\underline{f} - \underline{g} \\ \beta_{21}\overline{f} & \beta_{22}\underline{f} \end{bmatrix}, \quad A_4 = \begin{bmatrix} \beta_{11}\overline{f} & \beta_{12}\underline{f} - \overline{g} \\ \beta_{21}\overline{f} & \beta_{22}\underline{f} \end{bmatrix} \tag{9.76b}$$

$$B = \begin{bmatrix} 0 \\ \frac{1}{I_z} \end{bmatrix}, \quad E = \begin{bmatrix} \frac{C_f}{m} \\ \frac{a_f C_f}{I_z} \end{bmatrix} \tag{9.76c}$$

with $\beta_{11} = -\frac{C_f + C_r}{m}$, $\beta_{12} = -\frac{a_f C_f - a_r C_r}{m}$, $\beta_{21} = -\frac{a_f C_f - a_r C_r}{I_z}$, and $\beta_{22} = -\frac{a_f^2 C_f + a_r^2 C_r}{I_z}$. The weighting functions are given by

$$\mu_1(v_x(t)) = \mu_{11}(v_x(t))\mu_{21}(v_x(t)) \tag{9.77a}$$
$$\mu_2(v_x(t)) = \mu_{11}(v_x(t))\mu_{22}(v_x(t)) \tag{9.77b}$$
$$\mu_3(v_x(t)) = \mu_{12}(v_x(t))\mu_{21}(v_x(t)) \tag{9.77c}$$
$$\mu_4(v_x(t)) = \mu_{12}(v_x(t))\mu_{22}(v_x(t)) \tag{9.77d}$$

An actuator fault $f_a(t)$ affecting the controlled input $M_z(t)$ is considered here. Consequently, the faulty stabilizing moment provided by the controller is given by $M_z(t) = u_c(t) + f_a(t)$, where $f_a(t)$ can be considered as an UI to be estimated. No sensor faults $f_s(t)$ are considered. The fault-free reference model is

$$\dot{x}_r(t) = \sum_{i=1}^{4} \mu_i(v_x(t))\{A_i x_r(t) + E\delta_f(t)\} \tag{9.78}$$

The gains of the observer and the FTC are obtained by solving the LMI conditions given in Eq. (9.71). The time-varying longitudinal velocity and the steering angle are depicted in Fig. 9.12. It is noteworthy that because the longitudinal velocity is not constant, the system is nonlinear.

Fig. 9.13 shows that the state variables are correctly estimated, and that the trajectory tracking is efficient despite the action of the fault. As seen in Fig. 9.14, the fault magnitude estimation is also correct. The reference tracking results obtained with the FTC are depicted, in the $(x, y)$ plane, in Fig. 9.15. For comparison, the faulty vehicle states without FTC are also depicted in this figure. As shown in Fig. 9.13, the lateral velocities

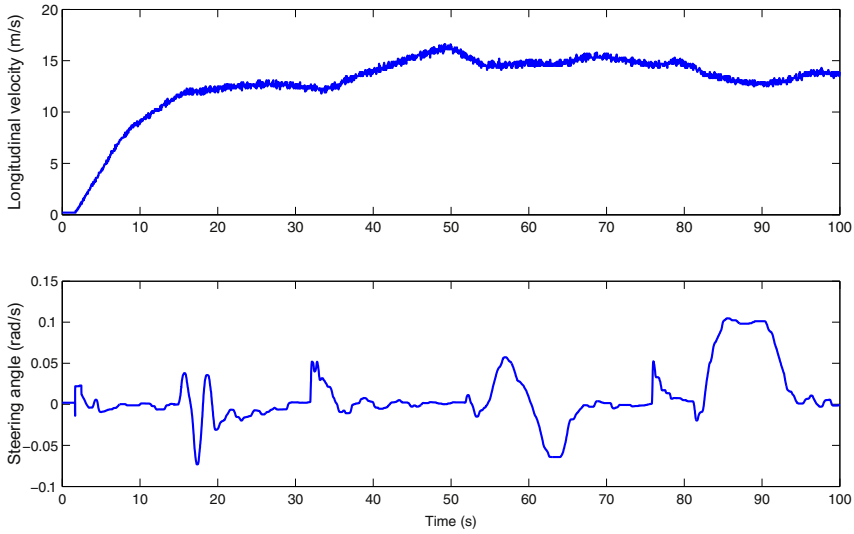


**FIG. 9.12** Longitudinal velocity and steering angle measurements.

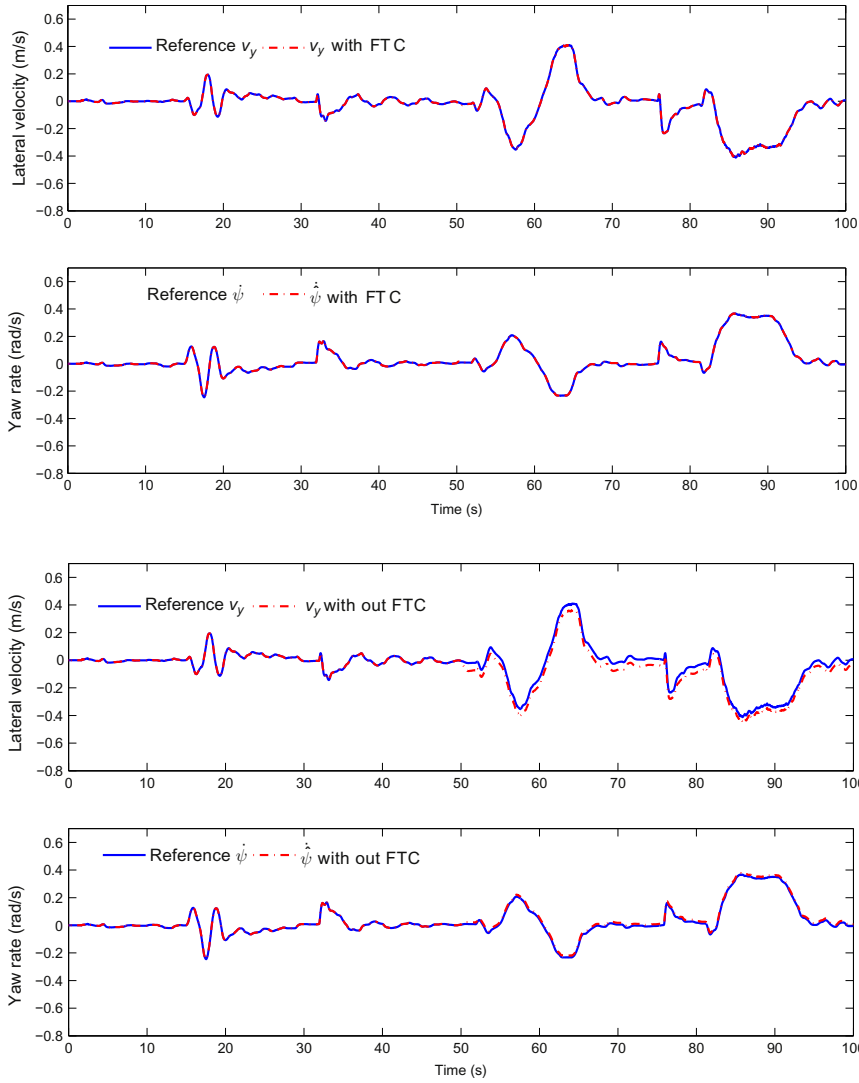


**FIG. 9.13** Reference states and faulty system states with and without fault-tolerant control.

$v_y(t)$ of the vehicle without FTC and of the reference model are different. Consequently, the faulty vehicle trajectory without FTC clearly deviates from the reference in Fig. 9.15. Thanks to the presented FTC, the fault estimate allows us to adapt the control law to the occurring fault to ensure a good reference trajectory tracking (see again Fig. 9.15), and thus improve the dynamic vehicle behavior. It clearly illustrates the benefits of the PM-based active FTC to cope with lateral vehicle stabilization.

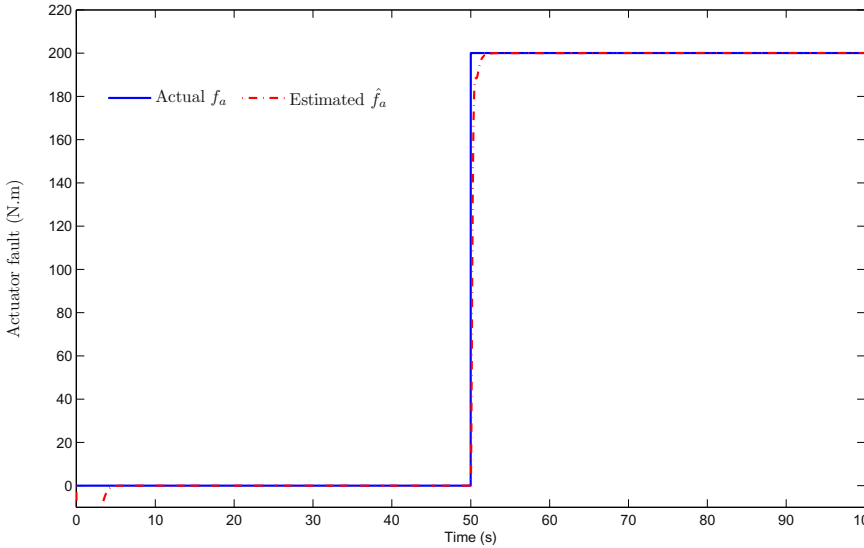


**FIG. 9.14** Fault and its estimate.

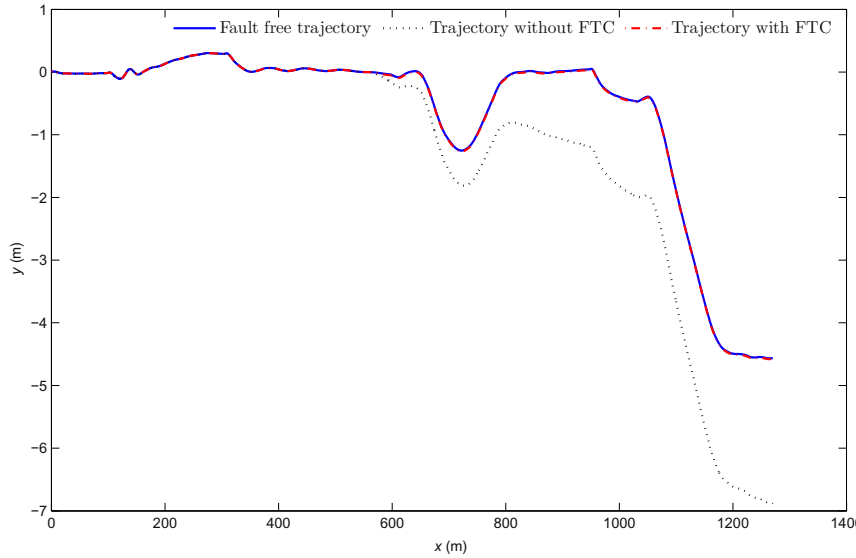


**FIG. 9.15** Reference trajectory (*blue line*) and faulty vehicle trajectory without FTC (*black dots*) and with FTC (*red dashed line*).

## 5.2 Partial Conclusion and Discussion

In this section the PM approach is employed to propose an efficient architecture for FTC. The design of the proposed FTC is based on LMI conditions. The structure of the FTC law aims to control the state of the faulty system in order to follow a reference state trajectory generated by a nominal reference model. This FTC can be modified in order to realize output trajectory tracking in the presence of faults. What has been done so far in this chapter requires the assumption that the premise variables $\xi(t)$ are measurable in real-time and fault-free. This approach can be extended for systems having faulty premise variables. For example, if the premise variables $\mu_i(\cdot)$ depend on the output of the system, then the sensor faults also affect these variables. Therefore, the reference model, the real system, and the observer do not share the same premise variables, and the design problem becomes more complex; but solutions are proposed in [29, 30].

# 6 OVERALL CONCLUSION

This chapter presents some results of the PM approach to cope with the modeling, the stability analysis, the state feedback control, the state and UI estimations, and finally, the FTC of nonlinear systems. The backbone of all the presented results is the capacity of the PM structure to represent nonlinearities in a selected operating range of the system. In this operating range, the nonlinear model of the system can be exactly rewritten as a PM, and thanks to this procedure, the specific analysis of each nonlinearity can be avoided. Notice, however, that the number of required submodels polynomially increases with the number of nonlinearities taken into consideration. It obviously causes numerical difficulties, and can be considered as the main limit of the approach. On the other hand, all proposed results are obtained provided that the system states remain in the selected operating range. Fortunately, in most real applications, the states are bounded, which means that the nonlinearities are also bounded, especially when the systems are in a closed loop.

Based on the polytopic modeling approach, stability conditions are formulated in terms of LMIs. In fact, even if the global PM is a nonlinear model, the Lyapunov method for stability analysis leads to LMI, due to the linearity of the submodels. According to the used Lyapunov function, less conservative conditions can be found. The relaxation of these conditions is today an open problem, in particular, for a large number of submodels.

The LMI stability conditions are then used to design robust state feedback controllers in order to stabilize the system at the origin. Desired closed-loop performances can be defined by specifying a desired decay rate, and the state feedback gain can also be optimized to reduce the impact

of a disturbance on the system state. In a similar way, observer designs providing an estimation of the state, even in the presence of UIs, are also exposed. These UIs can be, for example, faults acting on the actuators or sensors. The presented extended proportional integral observer (PIO) provides an estimation of the time of occurrence of the fault, as well as of its magnitude. Finally, by considering the benefits of modeling, control, and estimation advances for PM, we then propose designing a fault-tolerant controller fed with the simultaneous state and UI estimates. The benefits of the active fault-tolerant controller based on the PM approach are illustrated in an example consisting of the stabilization of the lateral dynamics of a vehicle.

## References

[1] C. Briat, LPV & Time-Delay Systems—Analysis, Observation, Filtering & Control, Advances in Delays and Dynamics Series, vol. 3, Springer, Heidelberg, 2015.
[2] R. Murray-Smith, T.A. Johansen, Multiple Model Approaches to Modeling and Control, Taylor and Francis, London UK, 1997.
[3] T. Takagi, M. Sugeno, Fuzzy identification of systems and its application to modeling and control, IEEE Trans. Syst. Man Cybernet. 15 (1) (1985) 116–132.
[4] D.J. Leith, W.E. Leithead, Analytic framework for blended multiple model systems using linear local models, Int. J. Control 72 (7/8) (1999) 605–619.
[5] P. Anjali, P. Deshpande, S.C. Patwardhan, Online fault diagnosis in nonlinear systems using the multiple operating regime approach, Ind. Eng. Chem. Res. 47 (17) (2008) 6711–6726.
[6] R. Orjuela, Contribution à l'estimation d'état et au diagnostic des systèmes représentés par des multimodèles (Ph.D. thesis), Institut National Polytechnique de Lorraine, France 2008 (In French), Available from: https://tel.archives-ouvertes.fr/tel-00359631v1.
[7] L. Ljung, Perspectives on system identification, Annu. Rev. Control 34 (1) (2010) 1–12.
[8] C. Hametner, M. Nebel, Operating regime based dynamic engine modelling, Control Eng. Pract. 20 (4) (2012) 397–407.
[9] R. Orjuela, B. Marx, D. Maquin, J. Ragot, Nonlinear system identification using heterogeneous multiple models, Int. J. Appl. Math. Comput. Sci. 23 (1) (2013) 103–115.
[10] A.A. Adeniran, S. El Ferik, Modeling and identification of nonlinear systems: a review of the multimodel approach—part 1, IEEE Trans. Syst. Man Cybernet. 47 (7) (2016) 1149–1159.
[11] S. El Ferik, A.A. Adeniran, Modeling and identification of nonlinear systems: a review of the multimodel approach—part 2, IEEE Trans. Syst. Man Cybernet. 47 (7) (2016) 1160–1168.
[12] A. Boukhris, G. Mourot, J. Ragot, Non-linear dynamic system identification: a multi–model approach, Int. J. Control 72 (7/8) (1999) 591–604.
[13] G.Z. Angelis, System Analysis, Modeling and Control With Polytopic Linear Models (Ph.D. thesis), Technology University Eindhoven, The Netherlands, 2001.
[14] K. Tanaka, H.O. Wang, Fuzzy Control System Design and Analysis: A Linear Matrix Inequality Approach, John Wiley and Sons, New-York, USA, 2001.
[15] H. Ohtake, K. Tanaka, H. Wang, Fuzzy modeling via sector nonlinearity concept, in: 9th IFSA World Congress and 20th NAFIPS International Conference, Vancouver, Canada, 2001.
[16] A.M. Nagy, G. Mourot, B. Marx, J. Ragot, G. Schutz, Systematic multi-modeling methodology applied to an activated sludge reactor model, Ind. Eng. Chem. Res. 46 (6) (2010) 2790–2799.

[17] K. Tanaka, T. Ikeda, H.O. Wang, Fuzzy regulators and fuzzy observers: relaxed stability conditions and LMI-based designs, IEEE Trans. Fuzzy Syst. 6 (2) (1998) 250–265.
[18] M. Chadli, Stabilité et Commande de Systèmes décrits par des Structures Multimodèles: Approche LMI (Ph.D. thesis), Institut National Polytechnique de Lorraine, France, 2002 (In French), Available from: https://tel.archives-ouvertes.fr/tel-00004605v1.
[19] H.O. Wang, K. Tanaka, M.F. Griffin, An approach to fuzzy control of nonlinear systems: stability and design issues, IEEE Trans. Fuzzy Syst. 4 (1) (1996) 14–23.
[20] H.D. Tuan, P. Apkarian, T. Narikiyo, Y. Yamamoto, Parameterized linear matrix inequality techniques in fuzzy control system design, IEEE Trans. Fuzzy Syst. 9 (2) (2001) 324–332.
[21] A. Sala, C. Arino, Asymptotically necessary and sufficient conditions for stability and performance in fuzzy control: applications of Polya's theorem, Fuzzy Sets Syst. 158 (24) (2007) 2671–2686.
[22] A. Kruszewski, R. Wang, T.M. Guerra, Nonquadratic stabilization conditions for a class of uncertain nonlinear discrete-time T-S fuzzy models: a new approach, IEEE Trans. Autom. Control 53 (2) (2008) 606–611.
[23] K. Guelton, T. Bouarar, N. Manamanni, Robust dynamic output feedback fuzzy Lyapunov stabilization of Takagi-Sugeno systems: a descriptor redundancy approach, Fuzzy Sets Syst. 160 (19) (2009) 2796–2811.
[24] S. Bezzaoucha, Commande tolérante aux défauts des systèmes non linéaires représentés par des modèles de Takagi-Sugeno (Ph.D. thesis), Université de Lorraine, France, 2013 (In French), Available from: https://tel.archives-ouvertes.fr/tel-00948345v1.
[25] S. Bezzaoucha, B. Marx, D. Maquin, J. Ragot, Nonlinear joint state and parameter estimation: application to a wastewater treatment plant, Control Eng. Pract. 21 (10) (2013) 1377–1385.
[26] R. Orjuela, B. Marx, D. Maquin, J. Ragot, State estimation for nonlinear systems using decoupled multiple model, Int. J. Model. Identif. Control 4 (1) (2008) 59–67.
[27] R. Orjuela, B. Marx, D. Maquin, J. Ragot, On the simultaneous state and unknown input estimation of complex systems via a multiple model strategy, IET Control Theory Appl. 3 (7) (2009) 877–890.
[28] D. Ichalal, Estimation et Diagnostic de Systèmes Nonlinéaires Décrits Par un Modèle de Takagi-Sugeno (Ph.D. thesis), Institut National Polytechnique de Lorraine, France, 2009 (In French), Available from: https://tel.archives-ouvertes.fr/tel-00454793v1.
[29] D. Ichalal, B. Marx, J. Ragot, D. Maquin, New fault tolerant control strategies for nonlinear Takagi-Sugeno systems, Int. J. Appl. Math. Comput. Sci. 22 (1) (2012) 197–210.
[30] D. Ichalal, B. Marx, D. Maquin, J. Ragot, Observer design and fault tolerant control of Takagi-Sugeno nonlinear systems with unmeasurable premise variables, in: G. Rigatos (Ed.), Fault Diagnosis in Robotic and Industrial Systems, iConcept Press Ltd, 2012.
[31] A.T. Nguyen, Outils de Commande Avancés pour les Applications Automobiles (Ph.D. thesis), Université de Valenciennes et du Hainaut-Cambrésis, 2013 (In French).
[32] Z. Yacine, D. Ichalal, N. Ait-Oufroukh, S. Mammar, S. Djennoune, Takagi-Sugeno observers: experimental application for vehicle lateral dynamics estimation, IEEE Trans. Control Syst. Technol. 23 (2) (2015) 754–761.
[33] A.M. Nagy, B. Marx, G. Mourot, G. Schutz, J. Ragot, Observers design for uncertain Takagi-Sugeno systems with unmeasurable premise variables and unknown inputs. Application to a wastewater treatment plant, J. Process Control 21 (7) (2011) 1105–1114.
[34] S. Georg, M. Müller, H. Schulte, Wind turbine model and observer in Takagi-Sugeno model structure, J. Phys.:Conf. Ser. 555 (1) (2014) 1–10.
[35] H. Schulte, E. Gauterin, Fault-tolerant control of wind turbines with hydrostatic transmission using Takagi-Sugeno and sliding mode techniques, Annu. Rev. Control 40 (2015) 82–92.
[36] D. Ichalal, B. Marx, J. Ragot, D. Maquin, Fault detection, isolation and estimation for Takagi-Sugeno nonlinear systems, J. Frankl. Inst. 351 (7) (2014) 3651–3676.

[37] C. Fantuzzi, R. Rovatti, On the approximation capabilities of the homogeneous Takagi–Sugeno model, in: 5th IEEE International Conference on Fuzzy Systems, New Orleans, LA, 1986.
[38] G. Cybenko, Approximations by superpositions of sigmoidal functions, Math. Control Signals Syst. 2 (4) (1989) 303–314.
[39] D. Liberzon, S. Morse, Basic problems in stability and design of switched systems, IEEE Control Syst. Mag. 19 (5) (1999) 59–70.
[40] D. Liberzon, Switching in Systems and Control, Birkhauser, Basel, Switzerland, 2003.
[41] L. Rodrigues, S. Boyd, Piecewise-affine state feedback for piecewise-affine slab systems using convex optimization, Syst. Control Lett. 54 (9) (2005) 835–853.
[42] V. Breschi, D. Piga, A. Bemporad, Piecewise affine regression via recursive multiple least squares and multicategory discrimination, Automatica 73 (2016) 155–162.
[43] J. Dong, G.-H. Yang, Robust control of continuous-time Markov jump linear systems, Automatica 44 (5) (2008) 1431–1436.
[44] P. Baranyi, D. Tikk, Y. Yam, R.J. Patton, From differential equations to {PDC} controller design via numerical transformation, Comput. Ind. 51 (3) (2003) 281–297.
[45] S. Boyd, L. El Ghaoui, E. Feron, V. Balakrishnan, Linear Matrix Inequalities in System and Control Theory, SIAM, Philadelphia, PA, USA, 1994.
[46] L. Wang, X. Liu, Parameter-varying state feedback control for discrete-time polytopic systems, Int. J. Syst. Sci. 42 (6) (2011) 997–1005.
[47] D.H. Lee, D.W. Kim, Relaxed LMI conditions for local stability and local stabilization of continuous-time Takagi-Sugeno fuzzy systems, IEEE Trans. Cybernet. 44 (3) (2014) 394–405.
[48] J. Maidens, M. Arcak, Reachability analysis of nonlinear systems using matrix measures, IEEE Trans. Autom. Control 60 (1) (2015) 265–270.
[49] J.K. Scott, P.I. Barton, Bounds on the reachable sets of nonlinear control systems, Automatica 49 (1) (2013) 93–100.
[50] M. Farza, K. Busawon, H. Hammouri, Simple nonlinear observers for on-line estimation of kinetic rates in bioreactors, Automatica 34 (3) (1998) 301–318.
[51] B. Marx, A descriptor Takagi-Sugeno approach to nonlinear model reduction, Linear Algebra Appl. 479 (2015) 52–72.
[52] A. Weinmann, Uncertain Models and Robust Control, Springer, Vienna, Austria, 1991.
[53] L.A. Mozelli, R.M. Palhares, F.O. Souza, E.M.A.M. Mendes, Reducing conservativeness in recent stability conditions of T-S fuzzy systems, Automatica 45 (6) (2009) 1580–1583.
[54] X. Liu, Q. Zhang, New approaches to $H_\infty$ controller designs based on fuzzy observers for T-S fuzzy systems via LMI, Automatica 39 (9) (2003) 1571–1582.
[55] F. Delmotte, T.M. Guerra, M. Ksantini, Continuous Takagi-Sugeno models: reduction of the number of LMI conditions in various fuzzy control design technics, IEEE Trans. Fuzzy Syst. 15 (3) (2007) 426–438.
[56] Q.T. Dinh, W. Michiels, S. Gros, M. Diehl, An inner convex approximation algorithm for BMI optimization and applications in control, in: IEEE Conference on Decision and Control (CDC), Maui, Hawaii, 2012.
[57] Q.T. Dinh, S. Gumussoy, W. Michiels, M. Diehl, Combining convex concave decompositions and linearization approaches for solving BMIs, with application to static output feedback, IEEE Trans. Autom. Control 57 (6) (2016) 1377–1390.
[58] M. Chilali, P. Gahinet, P. Apkarian, Robust pole placement in LMI regions, IEEE Trans. Autom. Control 44 (12) (1999) 2257–2270.
[59] L.A. Mozelli, R.M. Palhares, G.S.C. Avellar, A systematic approach to improve multiple Lyapunov function stability and stabilization conditions for fuzzy systems, Inf. Sci. 179 (8) (2009) 1149–1162.
[60] K. Tanaka, H. Ohtake, H.O. Wang, A descriptor system approach to fuzzy control system design via fuzzy Lyapunov functions, IEEE Trans. Fuzzy Syst. 15 (3) (2007) 333–341.

[61] J. Löfberg, YALMIP: a toolbox for modeling and optimization in Matlab, in: Computer Aided Control Systems Design, CACSD, Taipei, Taiwan, 2004, pp. 284–289.
[62] J.F. Sturm, Using SeDuMi 1.02, A Matlab toolbox for optimization over symmetric cones, Optim. Methods Softw. 11 (1) (1999) 625–653.
[63] D.G. Luenberger, Observers for multivariable systems, IEEE Trans. Autom. Control Act 11 (2) (1966) 190–197.
[64] M. Hou, R.J. Patton, Input observability and input reconstruction, Automatica 34 (6) (1998) 789–794.
[65] M. Darouach, M. Zasadzinski, S.J. Xu, Full-order observers for linear systems with unknown inputs, IEEE Trans. Autom. Control 39 (3) (1994) 606–609.
[66] S. Beale, B. Shafai, Robust control system design with a proportional integral observer, Int. J. Control 50 (1) (1989) 554–557.
[67] K. Busawon, P. Kabore, Disturbance attenuation using proportional integral observers, Int. J. Control 74 (6) (2001) 618–627.
[68] B. Shafai, C. Pi, S. Nork, Simultaneous disturbance attenuation and fault detection using proportional integral observers, in: American Control Conference, Anchorage, AK, 2002.
[69] Y. Xiong, M. Saif, Unknown disturbance inputs estimation based on a state functional observer design, Automatica 39 (8) (2003) 1389–1398.
[70] Y. Zhang, J. Jiang, Bibliographical review on reconfigurable fault-tolerant control systems, Annu. Rev. Control 32 (2) (2008) 229–252.
[71] J. Jiang, X. Yu, Fault-tolerant control systems: a comparative study between active and passive approaches, Annu. Rev. Control 36 (1) (2012) 60–72.
[72] R.J. Patton, P.M. Frank, R.N. Clark, Fault Diagnosis in Dynamic Systems—Theory and Application, Prentice Hall, Englewood Cliffs, NJ, USA, 1989.
[73] R.J. Patton, P.M. Frank, R.N. Clark, Issues of Fault Diagnosis for Dynamic Systems, Springer-Verlag, London, 1996.
[74] H. Noura, D. Theilliol, J.-C. Ponsart, A. Chamseddine, Fault-Tolerant Control Systems. Design and Practical Applications, Springer, London, UK, 2009.
[75] U. Kiencke, L. Nielsen, Automotive Control Systems, SAE International, Troy, MI, USA, 2000.